The effects of different speed skating push-off techniques on the mechanical power, power distribution and energy expenditure

T.P.J. Zuiker

Technische Universiteit Delft

TU Delft Delft University of Technology

Challenge the future

MSc thesis:

The effects of different speed skating push-off techniques on the mechanical power, power distribution and energy expenditure.

T.P.J. Zuiker
t.p.j.zuiker@student.tudelft.nl
student number: 4038363

July 9, 2014

Technische Universiteit Delft
Department of BioMechanical Engineering
Master BioMedical Engineering
Specialization BioMechatronics

Master Thesis advisor:
Prof. Dr. H.E.J. Veeger

Thesis committee:
Prof. Dr. H.E.J. Veeger, TU Delft
Ir. E. Van Der Kruk, TU Delft
Dr. J.J. De Koning, VU Amsterdam

Summary

The technique of speed skating is unique in comparison to other sports that require human propulsion. Skaters generate a forward velocity by pushing off sideways. The ideal push-off technique is a trade-off: a more sideward directed push-off facilitates power production, but a more forward directed push-off increases the transfers rate of push-off power into a forward velocity. The exact trade-off for the ideal push-off technique is unknown. Insight in the distribution of power in more than one direction and into the energy expenditure during different push-off techniques helps a speed skater in improving his or her push-off technique to the ideal push-off technique. This study quantifies the effect of different push-off techniques on the mechanical power, power distribution and energy expenditure. The study was limited to a group analysis of three push-off techniques: the small, self-chosen and wide push-off technique.

A three-dimensional power balance model was used to calculate the mechanical power in forward, sideward and upward components during speed skating. This model was driven by velocity and acceleration data, obtained by two synchronized measurement systems, and estimations of air and ice friction coefficients. The acceleration was measured by an Xsens MTI (Xsens) device and the velocity was calculated by fusing position (Local Position Measurement (LPM), Inmotio) and acceleration measurements (Xsens). The subject specific air and ice coefficients were estimated with position measurements (LPM) during gliding experiments. The mechanical power results were limited to the average mechanical powers of one representative stroke-cycle of skater and technique. The energy expenditure was estimated with steady state heart rate measurements (Polar) during speed skating.

This study proved a significant difference in forward power component, sideward power component and the total mechanical power between the push-off techniques studied, as well as the energy expenditure between the push-off techniques. The sideward power increased from small to self-chosen to wide push-off technique. In addition, this study showed that the change in total mechanical power was mainly due to the change in the sideward power component and that the energy expenditure in the self-chosen technique was the lowest. The relative mechanical efficiency, the ratio between total mechanical power and steady state heart rate, was significantly different for the three different push-off techniques. In addition, the relative mechanical efficiency increased from small to self-chosen to wide push-off technique. In summary, of the three push-off technique was the self-chosen push-off technique the most energy efficient push-off technique; this technique required the lowest energy expenditure for the required forward velocity. However, this technique was not the most mechanical efficient. The total mechanical power of the wide push-off technique was generated most mechanical efficient. This is because the more sideward push-off will make the push-off velocity less independent of the moving velocity and can be freely chosen to the optimal leg extension velocity, but introduces more 'wasted power' in non-effective movements for the performance.

The selected measurement method of this study can improve the current determination of the ideal push-off technique: analyzing the important trade-off between the mechanical efficiency and push-off orientation. This method be used to identify small changes between push-off technique in the mechanical efficiency and push-off orientation, and thus be used to improve speed skating performance. However, the measurement accuracy of this method requires to be improved further.

Contents

CHAPTER 1

Introduction

Speed skating is a very popular sport in The Netherlands. Almost everybody knows how to skate on ice. Fast skating requires an optimal combination of metabolic power, muscular strength and technique (Allinger and Van den Bogert 1997). The metabolic power and muscular strength can only be used maximally if the speed skating technique is optimal for these conditions. The technique of speed skating is unique in comparison to other sports that require human propulsion (Van Ingen Schenau and Cavanagh 1990, De Koning and Van Ingen Schenau 2008 and Fintelman 2011), as a speed skater generates a forward velocity by pushing off sideways (Figure 1.1). The sideward push-off enables the skater to have a longer push-off contact with the ice; the relatively low leg extension velocity is more or less independent of the forward velocity. This sideward push-off increases power generation capability during the high moving velocities of the skater. The downside of this sideward push-off is that the power generated by the skater is not only transferred into a forward motion, but also in a sideward motion. This sideward motion is undesirable for the skater's performance, because it will increase the travel distance due to a sinusoidal movement pattern.

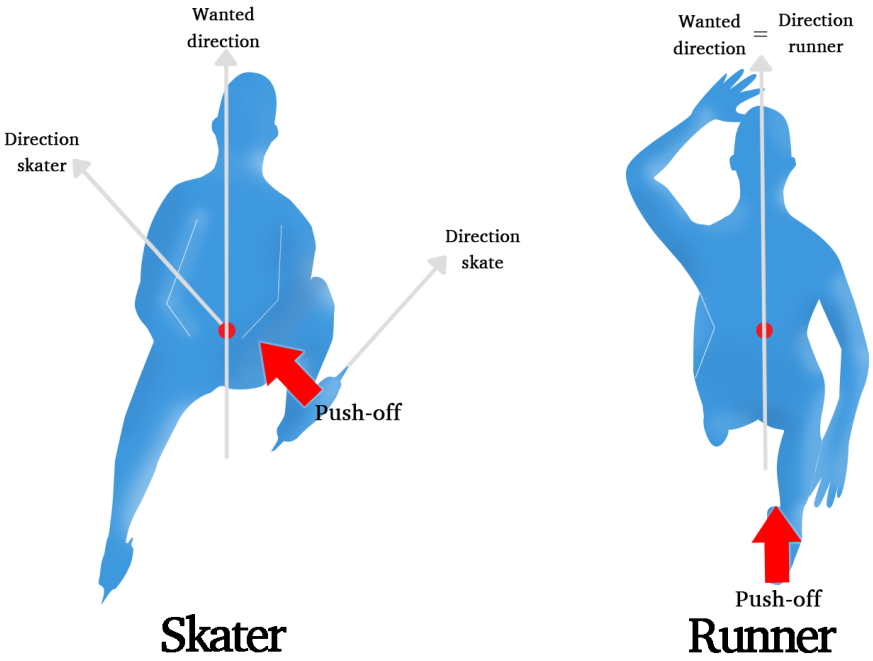

Figure 1.1: Comparison of push-off techniques between skating (left) and running (right).

Therefore, the ideal push-off technique is a trade-off in the push-off power distribution. A more sideward directed push-off facilitates power production, due to the increased independency of the extension velocity at high moving velocities. However, a more forward directed push-off increases the transfer rate of power into a forward velocity. Another important aspect of the ideal push-off technique is the energy expenditure of the skater. The push-off is the most energy efficient if the energy expenditure is minimal and the skater is still able to generate the required forward velocity. It

can be discussed if the minimal energy expenditure defines the ideal push-off technique. For example in cycling, may minimizing effort take precedence over minimizing energy expenditure (Chen et al. 1999), but it is assumed that low energy expenditure is very important factor to define the ideal push-off technique.

It is complex to determine the ideal push-off technique; it varies between speed skaters due the difference in body size, muscle properties, fatigue and fitness level (Zuiker 2013, Allinger and Van den Bogert 1997). The performance of the push-off technique is, during competitive trials, only judged on the motion of the speed skater in the forward direction (De Koning et al. 1994), while the motion of the speed skater in the other directions is also of importance for performance. The effectiveness of a push-off is related to the push-off angle between the skate and the ice (Van Ingen Schenau et al. 1985, De Boer et al. 1986 and Noordhof et al. 2013). However, the total mechanical power with respect to the forward direction has never been quantified between speed skaters or within different techniques. Insight in the distribution of power in more than one direction and into the energy expenditure during different push-off techniques helps a speed skater in improving his or her push-off technique to the ideal push-off technique.

The mechanical power exerted by speed skater has been investigated by De Koning (1991a, 1991b, 1992), De Boer et al. (1987a), Houdijk (2000b, 2001), Fintelman (2011) and Van der Kruk (2013b), but only Van Der Kruk analyzed the distribution of the push-off power. No studies made the distinction between different push-off techniques of the same speed skater. Van Ingen Schenau et al. (1983), De Boer et al. (1987b), Houdijk et al. (2000a) and De Koning et al. (2005) did analyze the energy expenditure in terms of oxygen uptake, but never made a distinction between different push-off techniques either.

Three push-off techniques are selected for the analysis of mechanical power, power distribution and energy expenditure. The three push-off techniques are the small, self-chosen and wide push-off technique. These three push-off techniques are very different. The small push-off is assumed to increase the transfer of power into the forward direction, while the wide push-off technique is assumed to facilitates power production more. The self-chosen technique is assumed to be a (self-chosen) trade-off between these two extremes.

The objective of this thesis is to provide insight into the distribution of the push-off power and energy expenditure by speed skaters applying different speed skating techniques. This insight can be used to quantify important observations, which can be used to improve and/or find the skaters personal ideal push-off technique.

1.1 Goal

To create this aforementioned insight, the following goal has been formulated:

> "Quantify the effects of different speed skating push-off techniques on the mechanical power, power distribution and energy expenditure"

Research Questions

Three research questions were defined to reach this main goal:

- What is the effect of different push-off techniques on the *mechanical power*?
- What is the effect of different push-off techniques on the *power distribution*?
- What is the effect of different push-off techniques on the *energy expenditure* ?

CHAPTER 2

Method

The human mechanical power was investigated using a three-dimensional version of the power balance model of Van Ingen Schenau (1981). The energy expenditure effects were investigated by measuring the steady state heart rate of the speed skater. The selection of the power and energy expenditure measurement methods and the selection of measurement devices are shown in Appendix A.

2.1 Experimental Design

Subjects
Ten subjects, 8 male and 2 female Dutch junior speed skaters, participated in this study. Six were members of the regional selection of Friesland, the other four were members of the regional selection of Zuid-Holland. The skaters were selected on their availability during the first week of December 2013 (Table 2.1).

Table 2.1: Descriptive characteristics of the subject

Parameter	**Male** ($n = 8$)	**Female** ($n = 2$)
Age	$19.4 \pm 1.5 year$	$20.5 \pm 0.5 year$
Body mass	$71.6 \pm 6.7 kg$	$60.0 \pm 1.0 kg$
Length	$181.4 \pm 5.8 m$	$171.5 \pm 3.5 m$
Personal record (PR) 3000m	$32.4 \pm 0.9 s$	$36.0 \pm 0.1 s$
Average velicity (PR 3000m)	$12.4 \pm 0.3 ms^{-1}$	$11.1 \pm 0.1 ms^{-1}$

Values are means ± standard deviation

Experiment
The quantification of the effects of different push-off techniques was limited to three distinct push-off techniques. The three different push-off techniques were the skaters' self-chosen (natural) push-off technique, a wide push-off technique and a small push-off technique. Each speed skater skated three series of six laps at submaximal performance level on the 400m indoor ice-track Thialf (Heerenveen, The Netherlands). The push-off technique was different for each series of laps, while the velocity was kept constant during all laps ($11.1 ms^{-1}$ male, $9.7 ms^{-1}$ female). The selected velocity indicated a submaximal performance level, which was lower than their personal record for approximately the same distance. The skaters were aided to maintain this constant velocity by projection of a moving dot on the ice rink (LaserTrainer, Figure 2.1). The speed skaters only skated on the inner lane of the two competition lanes and the data analyses was limited to the straight parts of the ice rink.

The speed skaters performed each of the three techniques sequentially, with a resting period of approximately 5 minutes between each technique. The first push-off technique was always the skater's self-chosen push-off technique. The order of the last two techniques was randomized to prevent order effects due to fatigue. The speed skater was instructed to use the width of one lane for the wide push-off technique and only half the width of the lane for the small push-off technique (Figure 2.2). There were no restrictions on the skater's self-chosen push-off technique. In all cases,

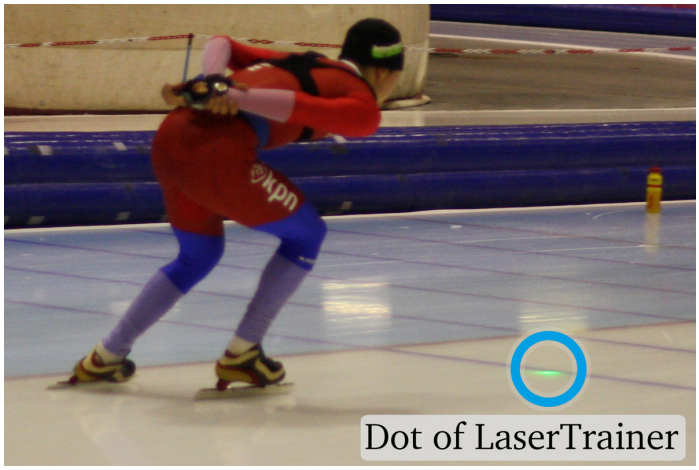

Figure 2.1: Speed skater during the experiment following the projected green dot of the laser-trainer on the ice.

the speed skater's personal technique was wider than the small technique and smaller than the wide technique.

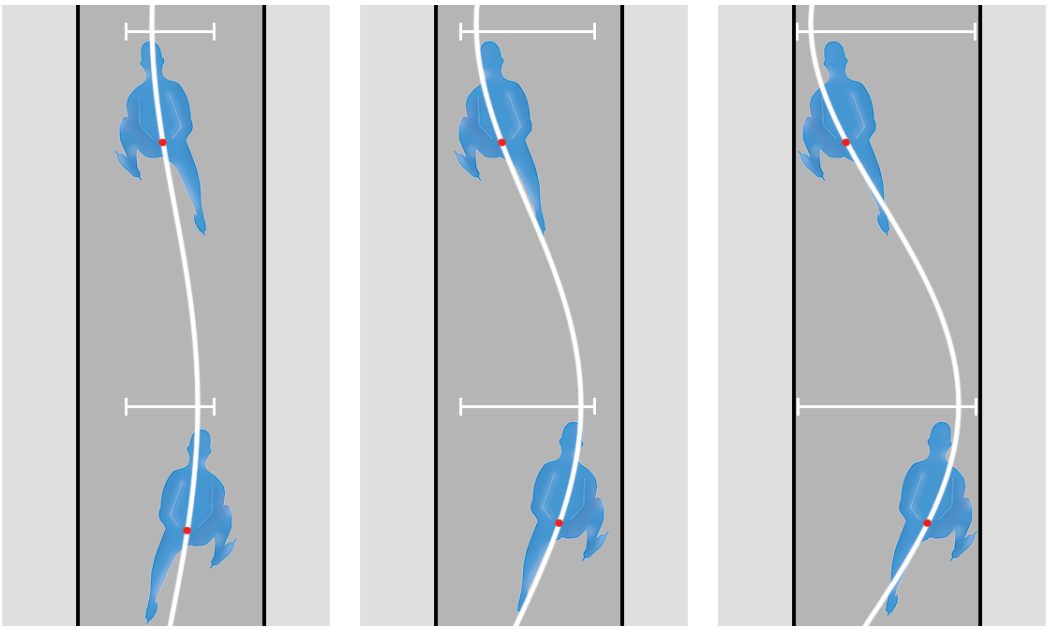

Figure 2.2: Definitions of the small (left), self-chosen (middle) and wide (right) push-off techniques in perspective of the width off one lane.

Mechanical Power

The mechanical power exerted by the speed skater was modeled by extending the one-dimensional power balance model of Van Ingen Schenau (1981). The model was driven by velocity (v) and acceleration (a) measurements and estimations of ice friction (μ) and air friction (k_1) coefficients (Equation (2.1) and Equation (2.2)). The model described the required mechanical power for movements in the forward, sideward and upward direction of the track orientation (Figure 2.3, Appendix A). The friction force was assumed only to be present in the sideward and forward direction. The distribution of the friction force was denoted by θ, the angle between the velocity in the forward and sideward direction. The ice and air friction coefficients were estimated in a separate gliding experiment. Appendix C describes the gliding experiment and the resulted air and ice friction coefficients for each speed skater.

$$
\begin{aligned}
P_x &= mv_x a_x + F_{fr} \cdot \cos(\theta) \cdot v_x \\
P_y &= mv_y a_y + F_{fr} \cdot \sin(\theta) \cdot v_y \\
P_z &= mv_z a_z + F_g \cdot v_z
\end{aligned} \tag{2.1}
$$

$$
F_{fr} = k_1 v^2 + \mu mg \tag{2.2}
$$

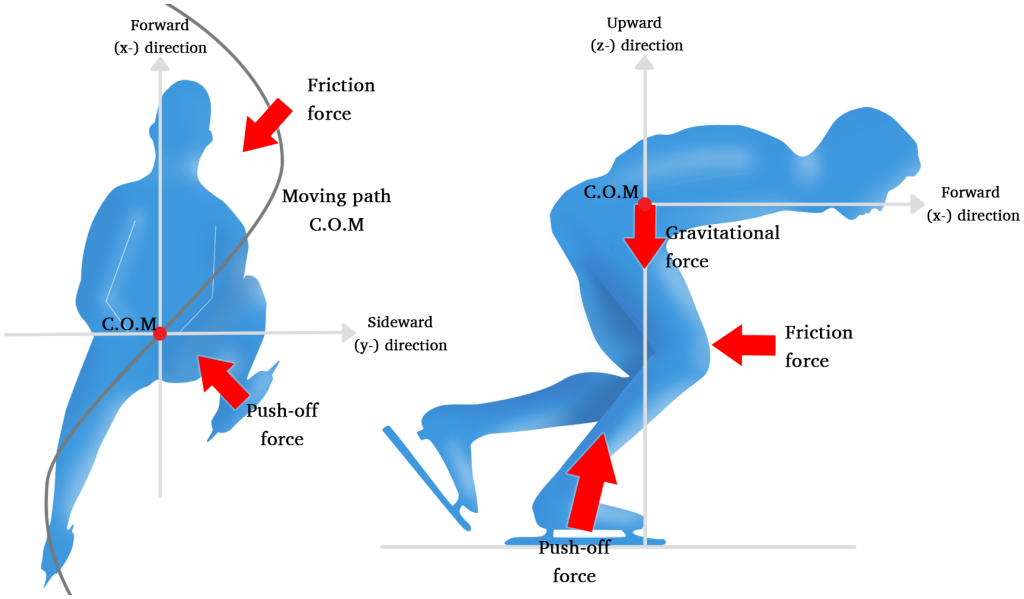

Figure 2.3: Top view (left) and side view (right) of the forces working on the speed skater in the track orientation.

Measurement Devices

Xsens MTi (Xsens MTi-28A53G35, Xsens) and LPM (Local Positioning Measurement, Inmotio) devices were used to measure the acceleration and position of the skater, respectively. The Xsens MTi device measured the acceleration, in three dimensions, of the skater, while the LPM device measured the position, in two dimensions. The Xsens MTi did also measured the orientation of the device to obtain the acceleration in the required track orientation. See Appendix A for more information of both devices. The required velocity was derived by fusion of the acceleration and position measurements. A synchronization protocol was used to synchronize the LPM device with the Xsens MTi device. The synchronization protocol included an extra stationary LPM sensor and stationary camera. The Xsens MTi and LPM devices were both placed on the back of the speed skater (Figure 2.4). The Xsens MTi sensor was placed on the skaters back using a belt. The battery and recording device for the Xsens MTi was also present in the belt. The LPM position sensor was placed on the skaters shoulders using a vest. The data of the LPM device were wirelessly stored on an external computer.

Energy Expenditure

The energy expenditure of the speed skaters was defined by the steady state heart rate of the skater. At submaximal performance levels, heart rate is linearly related to oxygen uptake for dynamic activities involving large muscle groups, and can provide a reasonable estimate of energy expenditure during exercise (Crouter et al. 2004). The heart rate of the speed skater was measured with a polar heart rate band (Polar, included with the LPM). The speed skater wore the polar heart rate band on his/her chest. The polar heart rate band was wirelessly connected and synchronized with the LPM.

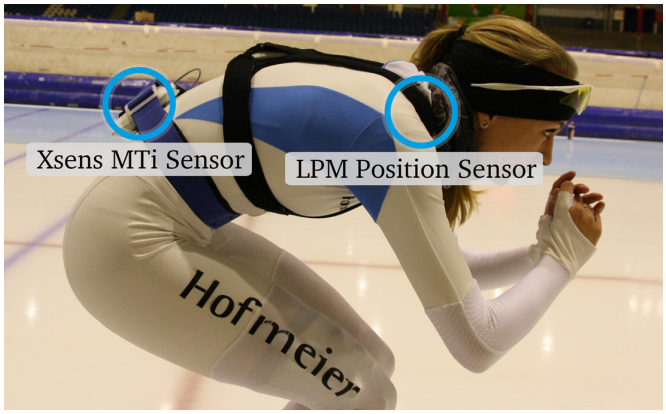

Figure 2.4: The placement of the Xsens MTi and LPM sensor on the back of the speed skater.

2.2 Post-Processing Method

The Xsens MTi measurements were stored in binary format on a data logger (AntiLog v5.1, Anti-Cyclone systems). The local accelerations, in three dimensions, and orientation of the device, with respect to the global reference, were extracted with the Xsens MTi low-level communication protocol documentation (Xsens Technologies 2010). The sample frequency of the Xsens MTi was set at 200Hz. The local accelerations were transformed to match the orientation of the three-dimensional power balance model. The known low accuracy of the indoor orientation measurement was corrected by optimizing the measured orientation of the device (Appendix D). The optimization was based on matching the average acceleration during each stroke-cycle, measured with the Xsens MTi device, with the average acceleration measured with the LPM device. There was no upward acceleration data available from the LPM device to match the Xsens acceleration for an optimization. Therefore, the average movement of the speed skater during one stroke-cycle, a cyclic pattern, was assumed at zero acceleration. For more information about the orientation and optimization technique, see Appendix D.

The LPM measurements were stored wirelessly on an external computer. The position measurements of both the stationary sensor and moving sensor (on the skaters back), and the heart rate data were exported using LPM software. The LPM device only measured the position of the skater in the forward and sideward orientation of the track orientation. The data were filtered by a linear filter and sampled at 200Hz with the available LPM software. The position data of the LPM data were differentiated to calculate the velocity. The velocity data was then processed and smoothed (running mean) to reduce large position measurement errors (Appendix B).

Following, the data of the LPM and Xsens devices were synchronized. A additional stationary camera and stationary LPM device were used for the synchronization. See Appendix E for the synchronization protocol and post-processing method.

Fusion of LPM and Xsens MTi data
Both the LPM position data and Xsens MTi acceleration were fused to improve the total accuracy of both the LPM and Xsens MTi velocity measurements separately (Appendix A). The acceleration was integrated per stroke-cycle, with the addition of the average velocity from the position data during the same stroke-cycle. The initial velocity in the upward direction was assumed zero.

Stroke-Cycle
The accelerations and velocity pattern during all stroke-cycles (on the straight parts of the ice rink) of one series of laps were averaged to create one representative acceleration and velocity pattern. Taking averages of the measured data reduces the measurement errors and subject-related variations. A stroke-cycle described sequentially one push-off with the left leg and one with the right leg and is the shortest repetitive movement pattern in speed skating on the straights. The resulted acceleration and velocity pattern during one stroke-cycle created a representative stroke-cycle for a skater with a specific push-off technique. See Appendix F for a detailed post-processing method to distinguish

the stroke-cycle on the straights and the method to takes averages of the velocity and acceleration during one stroke-cycle.

2.3 Data Analysis Method

The experimental results of 7 of the 10 speed skaters (5 male, 2 female) could be used for data analysis. Only the complete datasets, which include all three techniques of the subject, were selected. Some data were not complete due to malfunctioning of one or more devices (2 subjects) or due to withdrawal of subjects during the experiment (1 subject).

2.3.1 Mechanical Power and Power Distribution

The mechanical power and power distribution of each technique were analyzed on basis of one representative stroke-cycle per skater and their push-off technique. The average power during each representative stroke-cycle was used for analysis. This power was divided by the weight of the skater to enable comparison between different subjects.

The powers calculated with the three-dimensional power balance model were defined as *forward power*, *sideward power* and *upward power components* (Equation (2.1)) . The *forward power component* (P_x) and *sideward power component* (P_y) were defined as the resulted mechanical power due to friction force, velocity and the change of kinetic energy over time in x- or y-direction, respectively. The *upward power component* (P_z) was defined as the resulted mechanical power due to friction and gravitational force, velocity and change of kinetic energy over time in the z-direction (Equation (2.1) Figure 2.3). The *total mechanical power* of the skater was the sum of the forward, sideward and upward human power. *Power distribution* was defined as the mechanical power ratio between these directions.

Absolute Power
A negative power calculated with the power balance model indicated a force generated in the opposite direction as the velocity. Both the negative and positive power was thus generated by the skater. The power resulted with the power balance model was therefore made absolute (Equation (2.3)).

One exception was made for the forward power component: negative powers in the forward direction were assumed the result of overestimations of the friction forces and not due to a push-off force of the skater in the opposite direction as the velocity (Appendix G). The used friction coefficients described the average friction force during a stroke-cycle and could over or underestimate the friction force during the stroke-cycle. The observed negative power balances out the underestimations of the friction forces at another part of the stroke-cycle. The forward power component was therefore not made absolute. In conclusion, the forward, sideward and upward power components were analyzed as:

$$\begin{aligned} P_x &= \big(a_x + F_{fr} \cdot \cos(\theta)\big) \cdot v_x \\ P_y &= \big|\big(a_y + F_{fr} \cdot \sin(\theta)\big) \cdot v_y\big| \\ P_z &= |(a_z + 9.81) \cdot v_z| \end{aligned} \tag{2.3}$$

2.3.2 Energy Expenditure

The steady state heart rate of the skater was used to measure the energy expenditure. The steady state phase of the skaters heart rate was defined as the last minute of one series of laps. The average heart rate during this steady state heart rate was used to express the average energy expenditure of the skater during the push-off technique.

Heart rate measurements can not be used to define the absolute energy expenditure, but only the relative energy expenditure. The measured energy expenditure was therefore only used to describe the difference in energy expenditure between techniques.

2.3.3 Relative Mechanical Efficiency

The relative mechanical efficiency describes the ratio between the total mechanical power and the energy expenditure. The total mechanical power was, in contract to the otherwise used mechanical power, multiplied with the mass of the speed skater. The relative mechanical efficiency was used, instead of the (absolute) mechanical efficiency. The absolute mechanical efficiency required the absolute energy expenditure, which was not measured in this study. This study was limited to the relative energy expenditure.

2.4 Statistics

Differences between the three push-off technique groups were tested using an mixed between-within subjects design. The within-subject factor was the push-of technique (small, self-chosen and wide) and the between-subject factor was the gender (male and female). The significance level was set at $p<0.05$. The reported values represent the mean values of each technique group with the standard deviation as the spread around the mean of the representative stroke-cycle.

CHAPTER 3

Results

The male and female skaters rode at different predefined velocity of $11.1ms^{-1}$ and $9.7ms^{-1}$ respectively. There was a significance gender effect in velocity and acceleration results ($F(2,7) = 676$, $p < 0.001$ and $F(2,7) = 10.1$, $p = 0.02$, respectively), but no no significant interaction effect between push-off technique and gender for all other reported results.

As intended, the velocities did not differ between the three skating push-off techniques small, self-chosen and wide (Figure 3.1, $F(2,7) = 0.26$, $p = 0.78$). Furthermore, the forward acceleration did not differ between techniques (Figure 3.1, $F(2,7) = 4.02$, $p = 0.05$).

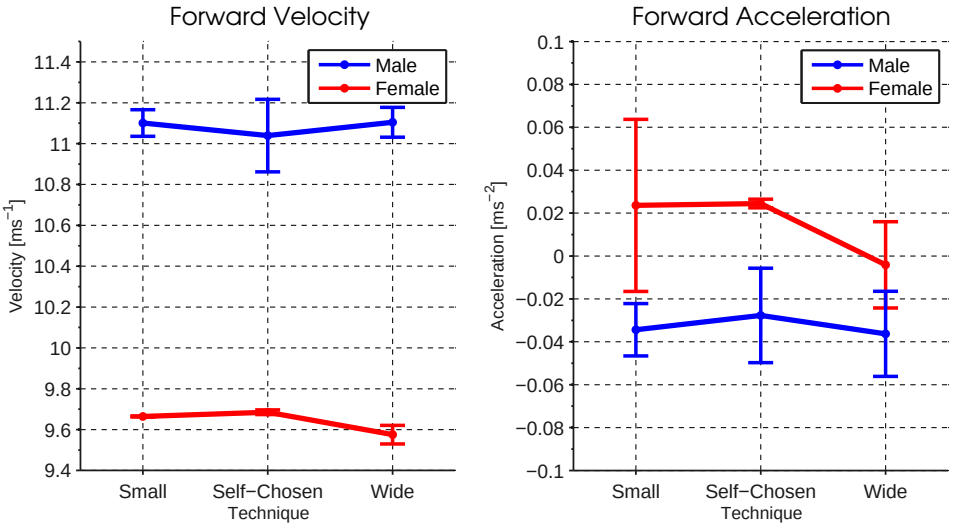

Figure 3.1: The average and standard deviation bar of the forward velocity and forward acceleration for different push-off techniques and gender.

3.1 Mechanical Power

Forward Power Component
The forward power component was slightly but significantly different between techniques (Figure 3.2, $F(2,7) = 4.26$, $p = 0.046$), but separately, the male and female subjects were not significant ($F(2,7) = 0.60$, $p = 0.57$ and $F(2,7) = 1.16$, $p = 0.38$, respectively). The male forward power component was $2.1 \pm 0.2 Wkg^{-1}$, $2.2 \pm 0.3 Wkg^{-1}$ and $2.1 \pm 0.3 Wkg^{-1}$ for small, self-chosen and wide technique, respectively. The female forward power component was $2.1 \pm 0.5 Wkg^{-1}$, $2.1 \pm 0.1 Wkg^{-1}$ and $1.8 \pm 0.3 Wkg^{-1}$ for small, self-chosen and wide technique, respectively.

Sideward Power Component
The sideward power component was significantly different between techniques (Figure 3.2, $F(2,7) = 19.53$, $p < 0.00$). The male and female skaters described the same pattern for the sideward

power component: an increasing power from small to self-chosen to wide. The male sideward power component was $2.3 \pm 0.3 W kg^{-1}$, $2.9 \pm 0.3 W kg^{-1}$ and $3.7 \pm 0.4 W kg^{-1}$ for small, self-chosen and wide technique, respectively. The female forward power component was $2.3 \pm 0.3 W kg^{-1}$, $2.8 \pm 0.1 W kg^{-1}$ and $3.4 \pm 0.3 W kg^{-1}$ for the small, self-chosen and wide technique, respectively.

Upward Power Component

The upward power component was not significantly different between techniques (Figure 3.2, $F(2,7) = 0.59$, $p = 0.56$). The male upward power component was $2.1 \pm 0.4 W kg^{-1}$, $1.9 \pm 0.5 W kg^{-1}$ and $1.7 \pm 0.3 W kg^{-1}$ for the small, self-chosen and wide technique, respectively. The female forward power component was $1.7 \pm 0.5 W kg^{-1}$, $1.7 \pm 0.3 W kg^{-1}$ and $1.7 \pm 0.7 W kg^{-1}$ for the small, self-chosen and wide technique, respectively.

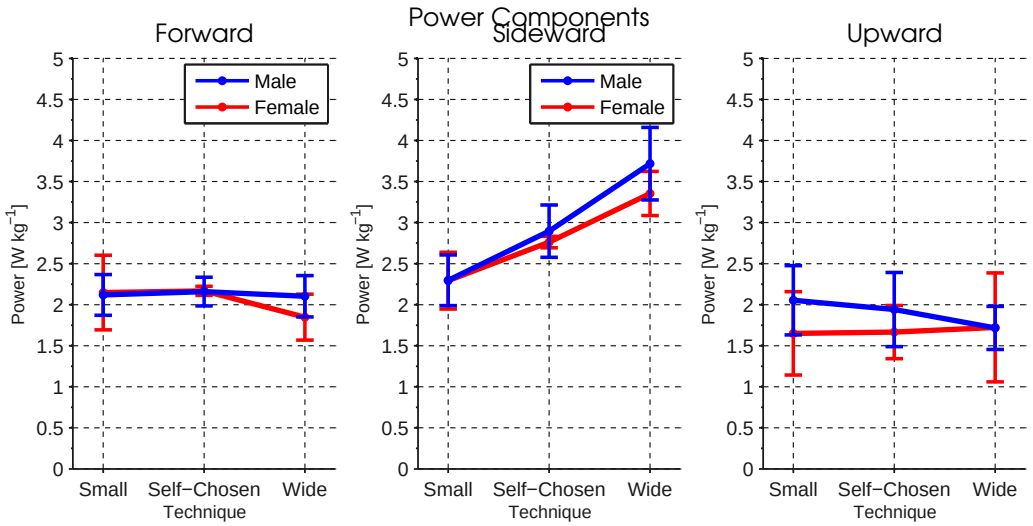

Figure 3.2: The average and standard deviation bar of the forward, sideward and upward power component for different push-off techniques and gender.

Total Mechanical Power

The total mechanical power was significantly different between techniques (Figure 3.3, $F(2,7) = 14.43$, $p < 0.00$). The male and female skaters described the same pattern; an increasing power from small to self-chosen to wide. The male total mechanical power was $6.5 \pm 0.4 W kg^{-1}$, $7.0 \pm 0.3 W kg^{-1}$and $7.5 \pm 0.2 W kg^{-1}$ for the small, self-chosen and wide technique, respectively. The female total mechanical power was $6.1 \pm 0.6 W kg^{-1}$, $6.6 \pm 0.4 W kg^{-1}$ and $6.9 \pm 1.2 W kg^{-1}$ for the small, self-chosen and wide technique, respectively.

3.2 Power Distribution

The forward power, sideward power and upward power ratios were significantly different between techniques (Figure 3.4, $F(2,7) = 16.25$, $p < 0.00$; $F(2,7) = 14.95$, $p < 0.00$ and $F(2,7) = 5.54$, $p = 0.02$, respectively). The power distribution for the small push-off technique was 33%, 36%, 30% for forward, sideward and upward power, respectively. The power distribution for self-chosen push-off technique was 31%, 42%, 27% for the forward, sideward and upward power, respectively. The power distribution for the wide push-off technique was 28%, 49%, 23% for forward, sideward and upward power, respectively. In all cases the sideward power remained the highest ratio and the upward the lowest ratio of the total mechanical power.

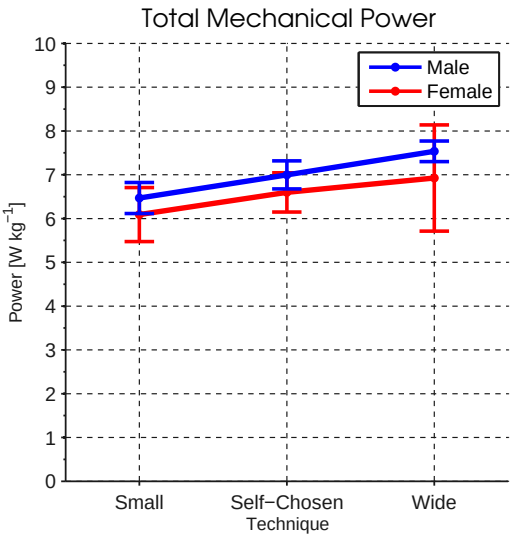

Figure 3.3: The average and standard deviation bar of the total mechanical power for different push-off techniques and gender.

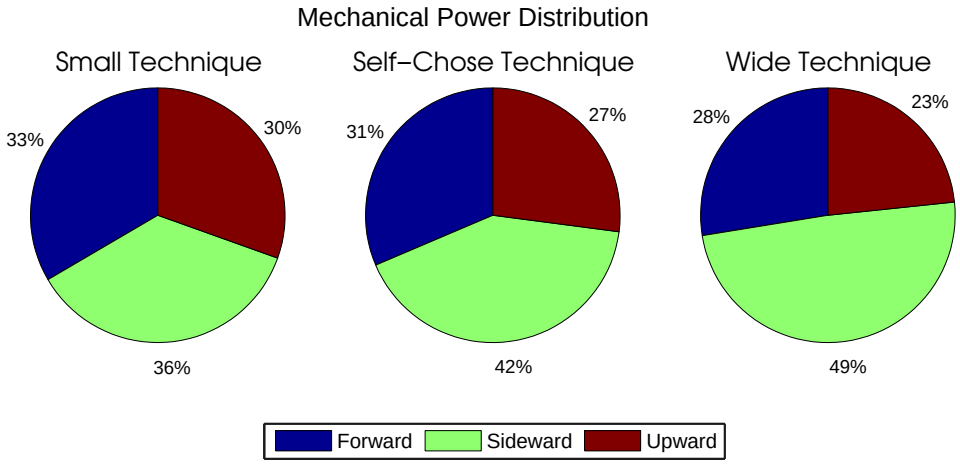

Figure 3.4: Power distribution of different push-off techniques and gender.

3.3 Energy Expenditure

The steady state heart rate was significantly higher for the small and wide technique with respect to the self-chosen technique (Figure 3.5, $F(2,7) = 13.25$, $p < 0.00$). The male and female skaters describe the same pattern: the steady state heart rate is higher for the not self-chosen techniques small and wide with respect to the self-chosen technique. The male steady state heart rate was $184.2 \pm 4.1 BeatsMin^{-1}$, $178.9 \pm 3.4 BeatsMin^{-1}$ and $185.3 \pm 5.4 BeatsMin^{-1}$ for the small, self-chosen and wide technique, respectively. The female steady state heart rate was $184.9 \pm 2.9 BeatsMin^{-1}$, $180.9 \pm 2.7 BeatsMin^{-1}$ and $185.9 \pm 6.6 BeatsMin^{-1}$ for the small, self-chosen and wide technique, respectively.

3.4 Relative Mechanical Efficiency

The relative mechanical efficiency was significantly different between techniques (Figure 3.6, $F(2,7) = 15.84$, $p < 0.00$). The male and female skaters described the same pattern: the relative mechanical efficiency increased from small to self-chosen to wide. The male relative mechanical

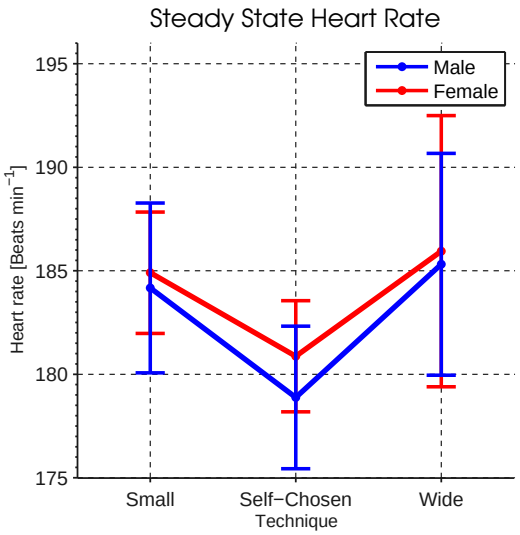

Figure 3.5: The average and standard deviation bars of the steady state heart rate for different push-off techniques and gender.

efficiency was 2.4 ± 0.3, 2.7 ± 0.3, and 2.8 ± 0.3 for the small, self-chosen and wide technique, respectively. The female relative mechanical efficiency was 2.4 ± 0.7, 2.6 ± 0.7, and 2.7 ± 0.9 for the small, self-chosen and wide technique, respectively.

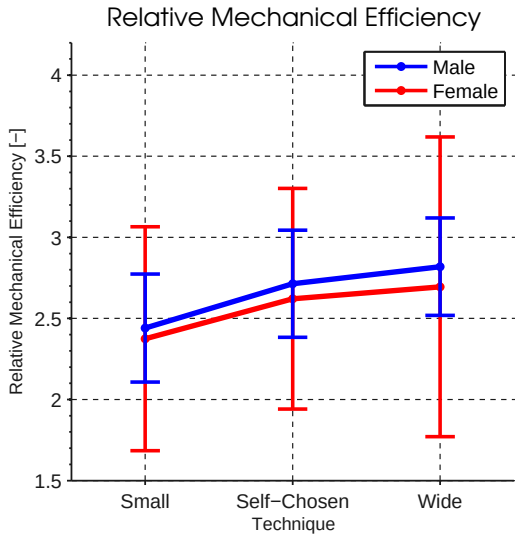

Figure 3.6: The average and standard deviation bar of the relative mechanical efficiency for different push-off techniques and gender.

CHAPTER 4

Discussion

4.1 Mechanical Power

Forward Power Component

The forward power component during the small push-off was slightly but significantly higher than the wide push-off ($p = 0.0047$). This was not expected, since the main factor of the forward power component, the velocity, was imposed to be constant for all push-off techniques. This significance is not present for the male and female subjects separately. The significant effect of the main factor and the non-significant effect for both genders separately is probably due to not even selection of male and female subjects and/or low number of subjects.

The forward power component was assumed to be mainly the effect of the friction forces: the forward acceleration was assumed zero, due to the constant imposed velocity. However, the average acceleration of the male and female skaters was not zero, but slightly higher ($-0.03 ms^{-2}$ for male, and $0.02 ms^{-2}$ for female). The non-zero acceleration had more impact on the forward power component than expected: a low forward acceleration of $0.03 ms^{-2}$ at $11.1 ms^{-1}$ does decrease the forward power component with 14%. The acceleration effect on the forward power component is also the reason why the forward power components of the male and female are almost equal, while the friction power should be different due to the different velocity. The forward power components of the male and female were almost equal, because the male acceleration is negative, while the female acceleration is positive.

The resulted forward power component is lower than found in literature. The male forward power component during the self-chosen push-off technique is approximately 45% lower by comparison of friction powers at approximately the same velocity (Table 4.1). The lower forward power component is lower due to the non-zero forward acceleration and the obtained air and ice friction coefficient. The air and ice friction estimation experiment resulted in lower air and ice friction coefficient in comparison to literature (Appendix C). The exact reason for the lower observed friction coefficients cannot be stated. The low air friction coefficient was most likely the result of passing skaters and different (smaller) knee and trunk angles. The ice friction coefficient was possibly lower due to gliding instead of skating.

Table 4.1: Friction power reported in literature

Literature	**Friction Power** $[W kg^{-1}]$	**Velocity** $[ms^{-1}]$
Forward Power (Self-Chosen)	2.2	11.1
Van Ingen Schenau et al. 1983	4.2	11.9
Van Ingen Schenau et al. 1985	4.3	11.4
De Koning et al. 2005	4.1	11.4
De Boer et al. 1986 (Elite)	4.4	12.0
De Boer et al. 1986 (Trained)	3.8	10.9

Sideward Power Component
The sideward power component increased significant from small to wide technique. This was also expected: a small push-off generates less sideward movement compared to the self-chosen technique, which results in a lower sideward power component. The opposite goes for the wide push-off, where the sideward power component is higher. To the knowledge of the author, this is the first study to include quantitative values of the sideward power component and therefore comparison with literature cannot be made.

Upward Power Component
The observed pattern in the upward power component is different for male and female speed skaters, but the observed values do not differ significant for different push-off techniques. No change in upward power was also expected, since the speed skater will try to minimize the friction regardless of the techniques. Reducing the upward movement does this.

De Boer and Nilsen (1989) observed that the body of the skater remains more or less constant during an entire stroke, but this was not observed in this study and also not in the studies of Fintelman (2011) and Van der Kruk (2013b). Fintelman observed accelerations up to 1.5 the gravitational force in the upward direction and Van Der Kruk observed that the 21% of the total mechanical power is used in upward direction. To the knowlage of the author, no exact upward power components values are known to compare the resulted upward power component.

Total Mechanical Power
The total mechanical power increased significantly from small to wide techniques. This increase was the result of the significantly change in forward and sideward power components. Since the forward power was just significant, is the effect mainly the result of the change in sideward power. This finding is in line with the expectation: a smaller sideward movement requires less mechanical power. The increasing values show the same pattern between the different genders.

The total mechanical power has only been reported in studies of Houdijk et al. (2000b) and Van der Kruk (2013b). Other studies have reported the mechanical power per joint as a function of time, but did not include average values during one push-off or stroke-cycle. Houdijk reported measurement of $234W$ for the average total mechanical power of one push-off with a velocity of $11.2ms^{-1}$, which is $468W$ per stroke-cycle. Van Der Kruk reported $348W$ and $352W$ of mechanical power per stroke-cycle with the use of a model ($v = \pm 9ms^{-1}$). This is $6.2Wkg^{-1}$, $4.6Wkg^{-1}$ and $4.7Wkg^{-1}$, respectively, when using an average weight of $75kg$. These values are in the same order of magnitude with respect to this study ($7.0Wkg^{-1}$), especially when taking into account that there were difference in velocity and assumed subject masses were used to compare these studies.

4.2 Power Distribution

The change in the power distribution ratio for forward, sideward and upward component were all significantly. This change was expected and mainly due to the significant change in sideward power component. During the wide push-off technique, the sideward power was almost 50% of the total mechanical power. Even during the small push-off technique represented the sideward power component the largest ratio of the total mechanical power. The ratio of the sideward power component is higher then expected, since the sideward power does not contribute directly to the skaters' performance. It was expected that the forward power component would be the largest ratio, as reported by Van der Kruk (2013b) (46%, 23%, 21% in the forward, sideward and upward direction, respectively). Houdijk et al. (2000b) reported both the total mechanical power, based on an inverse dynamic model, as well as the power to overcome friction (forward power), based on the power balance model. This ratio can be used to express the share of the forward power with respect to the total mechanical power. This creates a forward power ratio of 56%, which is higher then the the 31% reported for the self-chosen technique of this study. A possible cause for the low forward power ratio reported by Van Der Kruk and Houdijk is the also lower then reported forward power component. Correcting the resulted low forward power component to the in literature average value of $4Wkg^{-1}$ increases the forward power ratio to 45% and decreases the sideward power to 33%. The forward power component is now

more in line with the results of Van Der Kruk, and is also the highest component reported in both data.

The higher friction power does also change the total mechanical power of $7.0 Wkg^{-1}$ to $8.8 Wkg^{-1}$. The resulted total mechanical power will not anymore be in agreement with the results of Houdijk and Van Der Kruk. Since there is no data available on the sideward and upward power, is it not possible to evaluate whether one of the other mechanical power components is incorrect.

4.3 Energy Expenditure

The energy expenditure was the lowest for the self-chosen push-off technique and increased significantly for the small and wide technique. The lowest energy expenditure was indeed expected for the self-chosen technique, because the skater probably selected this technique because makes him/her skate the fastest with the least amount of energy. In addition, the other techniques require the skater to focus on implementing a new push-off technique, which also requires energy. Based on this study, it can only be concluded that the self-chosen technique is the most energy efficient push-off technique of the three to skate at the required velocity. However, it may well be that by practicing one of the other technique thoroughly, the energy expenditure would decrease on the long term and therefore this technique would become more energy efficient.

It was expected that the wide push-off technique would require more energy than the small push-off technique. Indeed, there is a difference, but this difference is minimal. A possible explanation for this relative high energy expenditure with the small push-off technique is the required faster leg extensions, because the small push-off is more dependent on the high forward velocity of the skater. Fast leg extension are expected to cost more energy than a lower leg extension. Another explanation of the high energy expenditure could be in the focus on the different technique: focusing on the small push-off technique could require more energy than focusing on the wide push-off technique.

The steady state heart rate during the self-chosen technique are in line with the results reported in speed skating (Table 4.2).

Table 4.2: Heart rate during speed skating reported in literature

Literature	**Heart rate** $[BeatsMin^{-1}]$	**Velocity** $[ms^{-1}]$
De Boer et al. (1987a)	174 ± 12.2	9.8
Van Ingen Schenau et al. (1983) elite	180 ± 10	12
Van Ingen Schenau et al. (1983) Trained	183 ± 10	10
Houdijk et al. (2000a) submaximal	161.0 ± 11.6	9.09
Houdijk et al. (2000a) maximal	172.5 ± 6.8	9.96

4.4 Relative Mechanical Efficiency

The relative mechanical efficiency was significantly different between the small and wide push-off technique and the mechanical efficiency increases from small to wide. This result was not expected. The skater's self-chosen technique was expected to be the most mechanically efficient, since the skater is most comfortable with this technique. The difference between the self-chosen and wide push-off technique was the result of an less increasing mechanical power with respect to the increase in heart rate. In conclusion, the total mechanical power for the wide push-off technique was generated the most efficient. This result does not mean that the wide push-off technique is also the most energy efficient technique to skate: that is the self-chosen technique. The wide push-off technique generates the total mechanical power most efficient, but 72% of the total mechanical power was used for sideward and upward movement and not for the wanted forward direction.

The result of the small push-off technique was expected, since it required higher energy expenditure, while the total mechanical power was lower. The forward power component was the highest for

the small push-off, which results in the most beneficial transfer of push-off power to the forward direction. However, this technique is not beneficial for the performance since it cost also more energy (heart rate). This low relative mechanical efficiency is interpreted to be the result of the fast leg extension velocity, which is assumed to be less energy efficient than a slow push-off velocity.

4.5 Limitations of the Study

4.5.1 Measurement Devices

Mechanical Power Measurements
The study was limited to a group analysis of the average mechanical power per representative stroke-cycle for each skater and techniques. This group analysis was chosen over individual analyses, because of inaccuracies in the measurements. In addition, the following steps were taken to reduce the errors in the measurements:

- The power loss of gained in each power component was assumed to be the result of pushing off of the speed skater or friction. In reality, power could also be increased or decreased by the transfer of power due to steering or a falling motion. These effects could not be separately analyzed and were therefore neglected.

- The acceleration in the track orientation required to be optimized, due to the low accuracy of the indoor ice-rink orientation measurements of the Xsens MTi device. The acceleration was therefore optimized. The optimization was based on matching the average acceleration during each stroke-cycle, measured with the Xsens MTi device, with the average acceleration measured with the LPM device. Zero acceleration during a stroke-cycle was assumed for the upward direction, since no data is available to match the upward acceleration.

- The position measurements of the LPM system and the optimized acceleration of the Xsens MTi required to be fused to reduce the velocity inaccuracy, which would be the result if the devices were used separately to calculate the velocity. It is unknown how much the optimization reduced the accuracy.

- The acceleration and velocity patterns of all stroke-cycles were averaged to a representative stroke-cycle to reduce the human inconsistencies and measurement and measurement errors. Therefore, it was not possible to analyze the difference in push-off between the same skater and technique.

- The study was limited to only the average mechanical power per representative stroke-cycle to reduce the effects of the inaccurate friction estimations during a stroke-cycle. Therefore, it was not possible to analyze the power difference during a single stroke-cycle.

Energy Expenditure Measurements
The heart rate of the skater is only an indication for the energy expenditure. There are limitations by measuring the energy expenditure with heart rate measurements:

- The average heart rate of the skater for the last minute of exercise was used as the steady state heart rate. There were still some fluctuations observed within the last minute of exercise, so the heart rate was not in steady state. The duration of the experiment per skating technique was too short to be able to determine if the average heart rate is equal to the steady state heart rate.

- The study was limited to the submaximal exercise conditions, since the heart rate has only a linear relation during submaximal exercises with the energy expenditure (Appendix A). This energy expenditure measurement cannot be used if the speed skaters performed a exercise at maximal conditions.

4.5.2 Measurement Methods

Mechanical Power Measurements
Two measurement method had been considered for the mechanical power measurement in the forward, sideward and upward component: the *force measurement method* and *power balance method* (Appendix A). The force measurement method was expected to be the most accurate method, but required special skaters, which were not operational for this study. Therefore, the power balance method was used. The accuracy of this method is limited by the need for friction force estimations. The estimation of friction forces have a high influence on the power outcome of the model and are difficult to obtain accurate during skating (Appendix A and Appendix C).

Energy Expenditure Measurements
There are two methods for measuring the energy expenditure during speed skating: measurement of the *heart rate* or *oxygen uptake* (Appendix A). The oxygen uptake measurement is assumed to have a higher accuracy of the energy expenditure measurement, since there is a direct linear relation between the energy expenditure and oxygen uptake. In addition, this measurement does also measure the absolute energy expenditure. The heart rate measurements can only be used to conclude on the difference in energy expenditure between the push-off techniques, because it only measures the relative change in energy expenditure. However, heart rate measurements were chosen over the oxygen uptake measurement, due to the simplicity of this measurement method. The heart rate measurement used the linear relation between oxygen uptake to determine the relative energy expenditure.

CHAPTER 5

Conclusion

This study was performed to analyze the effects of different push-off techniques on the mechanical power, power distribution and energy expenditure of the speed skater. The differences in sideward and upward components of mechanical power and power distribution had been assumed, but never quantified. The quantification of the mechanical power in this study revealed a significant difference in the total mechanical power between the different push-off technique. This difference in total mechanical power was mainly the result of the significant change in the sideways power component. In addition, this study also concluded that the power distribution in forward, sideward and upward ratio were all significantly different between the push-off techniques.

Of the three investigated push-off technique was the self-chosen push-off technique the most energy efficient push-off technique. Although this technique was not the most mechanical efficient, it had the lowest energy expenditure for the required forward velocity. The sideward push-off technique was the most mechanical efficient: the total mechanical power was generated the most efficient. However, most of this obtain mechanical power is not directed in the wanted forward direction, but 'wasted' in sideward and upward movements. Thus, solely based on the energy expenditure, the self-chosen push-off technique would be the ideal push-off technique. As stated in the introduction, the ideal push-off technique is a trade-off in push-off orientation: a more sideward direction push-off increases the mechanical efficiency, while a more forward directed push-off increases the ratio total mechanical power direction in the wanted forward direction. The optimal leg extension velocity can explain this trade-off. The power generation of the leg has an optimal leg extension velocity at which the most power can be generated (Zuiker 2013). A more sideways push-off will make the push-off velocity less independent of the moving velocity and can be freely optimized to the optimal leg extension velocity, but introduces more 'wasted' power in non-effective movements for the performance.

To achieve the maximal velocity, the skater needs to adjust the push-off to his/here maximal metabolic power and muscular strength available. The measurement method described in this study can be used to improve the determination of an individual ideal push-off technique. The push-off technique does not have to be quantified anymore on basis of the performance (lap time/velocity) or push-off angle, but on the important trade-off between the mechanical efficiency and push-off orientation. This method can be used to identify small changes during the push-off technique in the mechanical efficiency and push-off orientation and state whether the small changes improve or deteriorate the push-off technique. One important note requires to be made for determine the ideal push-off technique: these small changes can only be observed if the current measurement accuracy is improved.

CHAPTER 6

Future Work

Measurement inaccuracies limited this study to a group analysis of the average mechanical power per representative stroke-cycle for each skater and technique. Improvement of the current measurement devices and/or method can extend the analysis of the power distribution of the skater. Small changes during the push-off technique can only be quantified with more accurate measurement devices. Analyzing separate power distribution pattern during single stroke-cycles can help the skater improve his/her ideal push-off technique. Exploring research on this is already being conducted on the mechanical power distribution during the representative stroke-cycle of the different push-off techniques (Appendix G). These results show, for example, the timing of the skater and the effects of friction during a stroke-cycle. These results are not included into this study, due to the inaccuracies in the friction estimation.

Mechanical Power Measurements
The used measurement devices were not optimal and should be improved or replaced by more accurate measurement devices. The two-dimensional LPM measurement system, that is currently used in speed skating, was not sufficient for the measurement, since it cannot be used to calculate velocity and acceleration accurate during short intervals (during the stroke-cycle). In addition, a two-dimensional measurement system is not sufficient to capture all mechanical power of the skater. More than 23% of the total mechanical power is used in the not measured upward direction. The orientation measurementz of the Xsens MTi device were not accurate for indoor ice rink measurements. The accuracy of the orientation measurements requires to be increased by, for example, and custom speed skating Kalman filter. A single three-dimensional high precision position measurement system would be ideal for further measurements, as it would remove all the previously describe steps to improve the accuracy of the currently used measurement devices and it can measure both the acceleration and velocity.

The power balance model still requires accurate estimations of the friction forces. The current estimation the friction forces (gliding experiment) did not resulted in the same values are reported in literature. The estimation of the friction forces should be improved by also measuring multiple gliding sections with different knee and trunk angles and without any other skaters on the ice-rink. The obtained personal friction coefficients could be used with the general air friction estimations model of Van Ingen Schenau and be made dependent on trunk angle, knee angle, and velocity.

Mechanical Power Methods
For future studies, the force measurement method would be preferred over the in this study used power balance method to measure the mechanical power. This method will measure the mechanical power directly, and does not require friction estimations, but it will require accurate and stable force measurements, and in addition include a three dimensional high precision position measurement system.

The power estimation method and force estimation method combined can measure the friction forces during speed skating. This can be used to improve the estimations of the friction forces during speed skating, instead of using estimations of static gliding or wind tunnel experiments.

Energy Expenditure
Measuring the energy expenditure with heart rate measurements can be improved by extending the duration of the speed skating experiment. This will improve the steady state heart rate measurements.

The oxygen uptake measurement should be used if the energy expenditure requires to be measured more accurately and also to determine the actual mechanical efficiency, instead of the relative mechanical efficiency. Besides the energy expenditure, the required effort of the skater is an important determinant for the ideal push-off technique. According to Chen et al. (1999) minimizing effort does take precedence over minimizing energy expenditure. The subject could thus be more comfortable (least effort) by performing a task with a higher than minimal energy expenditure. If this conclusion also hold true for speed skating can be conducted in a further measurement by including effort measurements.

CHAPTER 7

Acknowledgments

During this graduation thesis I encountered a lot of obstacles, but in the end I managed to overcome all obstacles and present to you this thesis. Special thanks goes out to Prof. Dr. H.E.J. Veeger, Dr. Ir. A.L. Schwab, Ir. O den Braver and Ir. E. van der Kruk for their guidance, advice and support during all stages of my master thesis. Also, I want to to thank A. van der Wulp (Innosportlab) and Thialf Heerenveen for the use of their facilities. Futhermore, I want to thank Ir. J. Huijbers, L. Vogelpoel MSc, Ir. B. Koopman, and Ir. J. Groen for proof-reading parts of my thesis. Last but not least I want to thank my friends, family and especially Karen for their time, patience, support, and encouragement during my graduation.

CHAPTER 8

Bibliography

Allinger, T.L. and A.J. Van den Bogert (1997). “Skating technique for the straights, based on the optimization of a simulation model”. eng. In: *Med Sci Sports Exerc* 29.2, pp. 279–286.

Chen, Baoyuan, N.L. Jones, and K.J. Killian (1999). “Is there a conflict between minimizing effort and energy expenditure with increasing velocities of muscle contraction in humans?” In: *The Journal of Physiology* 518.3, pp. 933–940.

Crouter, S.E., C. Albright, and D.R. Bassett (2004). “Accuracy of Polar S410 Heart Rate Monitor to Estimate Energy Cost of Exercise”. In: *Medicine & Science in Sports & Exercise* 36.8, pp. 1433–1439.

De Boer, R.W. and KL Nilsen (1989). “The gliding and push-off technique of male and female Olympic speed skaters”. In: *International Journal of Sport Biomechanics*, pp. 119–134.

De Boer, R.W., P. Schermerhorn, J. Grademan, and G.J. Van Ingen Schenau (1986). “Characteristic stroke mechanics of elite and trained male speed skaters”. In: *Int J Sport ...* Pp. 175–185.

De Boer, R.W., J. Cabri, W. Vaes, J.P. Clarijs, A.P. Hollander, G. De Groot, and G.J. Van Ingen Schenau (1987a). “Moments of force, power, and muscle coordination in speed-skating.” In: *International journal of sports medicine* 8.6, pp. 371–8.

De Boer, R.W., E. Vos, and W. Hutter (1987b). “Physiological and biochemical comparison of roller skating and speed skating on ice”. In: *European Journal of Applied Physiology and Occupational Physiology* 56.5, pp. 562–569.

De Koning, J.J. and G.J. Van Ingen Schenau (2008). “Performance-Determining Factors in Speed Skating”. In: *Biomechanics in Sport*, pp. 232–246.

De Koning, J.J., G. De Groot, and G.J. Van Ingen Schenau (1991a). “Coordination of leg muscles during speed skating”. In: *Journal of Biomechanics* 24.2, pp. 137–146.

De Koning, J.J., G. De Groot, and G.J. Van Ingen Schenau (1991b). “Speed Skating the Curves: A Study of Muscle Coordination and Power Production”. In: *International Journal of Sport Biomechanics* 7, pp. 344–358.

De Koning, J.J., G. De Groot, and G.J. Van Ingen Schenau (1992). “Ice friction during speed skating”. In: *Journal of Biomechanics* 25.6, pp. 565–571.

De Koning, J.J., F.C. Bakker, G. De Groot, and G.J. Van Ingen Schenau (1994). “Longitudinal Development of Young Talented Speed Skaters - Physiological and Anthropometric Aspects”. English. In: *Journal of Applied Physiology* 77.5, pp. 2311–2317.

De Koning, J.J., H. Houdijk, G. De Groot, and M.F. Bobbert (2000). “From biomechanical theory to application in top sports: the Klapskate story”. In: *Journal of Biomechanics* 33.10, pp. 1225–1229.

De Koning, J.J., C. Foster, J. Lampen, F. Hettinga, and M.F. Bobbert (2005). “Experimental evaluation of the power balance model of speed skating”. In: *Journal of Applied Physiology* 98.1, pp. 227–233.

Farringdon, J. and D. Wolf (2006). *Does Heart Rate Predict Energy Expenditure? Yes, but ...*

Fintelman, D.M. (2011). *MSc report Simplest Skater Model*. Tech. rep. Technische Universiteit Delft.

Gemser, H., J.J. De Koning, and G.J. Van Ingen Schenau (1999). “Handbook of Competitive Speed Skating”. In:

Houdijk, H., E.A.M. Heijnsdijk, J.J. De Koning, G. De Groot, and M.F. Bobbert (2000a). “Physiological responses that account for the increased power output in speed skating using klapskates”. In: *European Journal of Applied Physiology* 83.4-5, pp. 283–288.

Houdijk, H., J.J. De Koning, G. De Groot, M.F. Bobbert, and G.J. Van Ingen Schenau (2000b). “Push-off mechanics in speed skating with conventional skates and klapskates”. In: *Medicine and Science in Sports and Exercise* 32.3, pp. 635–641.

Houdijk, H., A.J. Wijker, J.J. De Koning, M.F. Bobbert, and G. De Groot (2001). “Ice friction in speed skating: can klapskates reduce ice frictional loss?” eng. In: *Med Sci Sports Exerc* 33.3, pp. 499–504.

Keim, N.L., C.A. Blanton, and M.J. Kretsch (2004). “America’s obesity epidemic: measuring physical activity to promote an active lifestyle.” In: *Journal of the American Dietetic Association* 104.9, pp. 1398–409.

Levine, J.A. (2007). “Measurement of energy expenditure”. English. In: *Public Health Nutrition* 8.7a, pp. 1123–1132.

Noordhof, D.A., C. Foster, M.J.M Hoozemans, and J.J. De Koning (2013). “Changes in speed skating velocity in relation to push-off effectiveness”. In: *International Journal of Sports Physiology and Performance* 8.2, pp. 188–194.

Van Ingen Schenau, G.J. (1981). “A power balance applied to speed skating”. PhD thesis.

Van Ingen Schenau, G.J. (1982). “The influence of air friction in speed skating”. In: *Journal of Biomechanics* 15.6, pp. 449–458.

Van Ingen Schenau, G.J. and P.R. Cavanagh (1990). “Power equations in endurance sports”. In: *Journal of Biomechanics* 23.9, pp. 865–881.

Van Ingen Schenau, G.J., G. De Groot, and A.P. Hollander (1983). “Some technical, physiological and anthropometrical aspects of speed skating”. In: *European Journal of Applied Physiology and Occupational Physiology* 50.3, pp. 343–354.

Van Ingen Schenau, G.J., G. De Groot, and R.W. De Boer (1985). “The control of speed in elite female speed skaters”. In: *Journal of Biomechanics* 18.2, pp. 91–96.

Van der Kruk, E. (2013a). *Literature Thesis: Smooth Measuring*. Tech. rep.

Van der Kruk, E. (2013b). “Modelling and Measuring 3D movements of a speed skater.” Master Thesis. Technical University Delft.

Xsens Technologies (2010). *MT Low-Level Communication Protocol Documentation*. Tech. rep.

Zuiker, T.P.J. (2013). *Literature study: Leg power profile for an optimal performance?* Tech. rep. Technical University Delft.

APPENDIX A

Selection of Methods and Devices

Multiple methods can be selected to measure the mechanical power and energy expenditure of different push-off techniques. This chapter explains these different methods and the devices for both the mechanical power and energy expenditure measurement methods.

A.1 Mechanical Power Measurement

A.1.1 Method Selection

There are roughly two methods for mechanical power measurements during speed skating:

- Force measurements method
- Power balance model method

Force measurements
The force measurement method measures the push-off force and velocity of the speed skater to calculate the mechanical power. Force measurements were performed, among others, in the study of De Koning (1991a, 1991b, 1992), De Boer et al. (1987a), Houdijk (2000b, 2001), Fintelman (2011) and Van der Kruk (2013b) by use of an instrumented skate. They all used special force measurement skates to measure the push-off force. De Koning, De Boer and Houdijk used conventional force measurement skates and video analysis to measure the push-off force and the velocity. These studies were focused on the mechanical power in the hip, knee and ankle joint of the self-chosen push-off technique. Fintelman and Van Der Kruk used klap force measurement skates and a position measurement system to measure the push-off force and velocity and were primarily focused on the total mechanical power during the self-chosen push-off technique. However, Van Der Kruk also calculated the power distribution in forward, sideward and upward direction.

Power balance model
The power balance model method calculates the mechanical power of the skater with the power balance model and is common for mostly all power measurements during peed skating (Van Ingen Schenau (1982, 1983), De Boer (1986, 1987b), Houdijk (2000a, 2000b, 2001) and De Koning 1991b, 2005, 2008). All reported studies were limited to the average mechanical power during one or more laps. The power balance model is developed by Van Ingen Schenau (1981). The power balance model calculates the mechanical power by estimating the air and ice friction and requires measurements of the velocity during the experiment. The model is one-dimensional; only the forward mechanical power can be estimated. Therefore, the power balance model of Van Ingen Schenau should be extended to model the human power in all three directions.

Method Selection
The force measurement method was preferred to measure the effects of different push-off techniques on the mechanical power. This method is assumed to be the most accurate measurement, because the this method does not require estimations of the friction forces. These estimations only describe the average friction forces during one or more laps, and not at a exact moment during a push-off.

Unfortunately, it was not possible to use the klap force measurement skates for this research. Trial experiments have revealed structural problems to store the force data and the storage device was not stable during the skating exercise. Therefore, the extended three-dimensional power balance model was selected for measurements.

A.1.2 Three-dimensional Power Balance Model

The power balance model of Van Ingen Schenau simplifies the speed skater as a one-dimensional point mass in only the forward direction. The model describes the balance between the power output at one side and the friction power and change of the speed skaters' motion at the other side (Equation (A.1)). The change of the speed skaters' motion is defined as the rate of change of kinetic energy over time, which is a function of velocity and acceleration during the experiment.

$$\begin{aligned} P_o &= P_f + \frac{d}{dt}\left(\frac{1}{2}mv^2\right) \\ P_o &= P_f + mva \end{aligned} \tag{A.1}$$

The power balance model can be extended to also describe the power balance of the skater also in the sideward (y) and upward (z) direction. The upward direction is aligned with the gravitational force and the sideward direction is perpendicular to the forward and sideward directions (Figure A.1. Friction works also against the skater in the sideward and upward direction and the upward direction also includes the gravitational force. The three-dimensional power balance model is:

$$\begin{aligned} P_x &= mv_x a_x + P_{fr_x} \\ P_y &= mv_y a_y + P_{fr_y} \\ P_z &= mv_z a_z + P_{fr_z} + P_g \end{aligned} \tag{A.2}$$

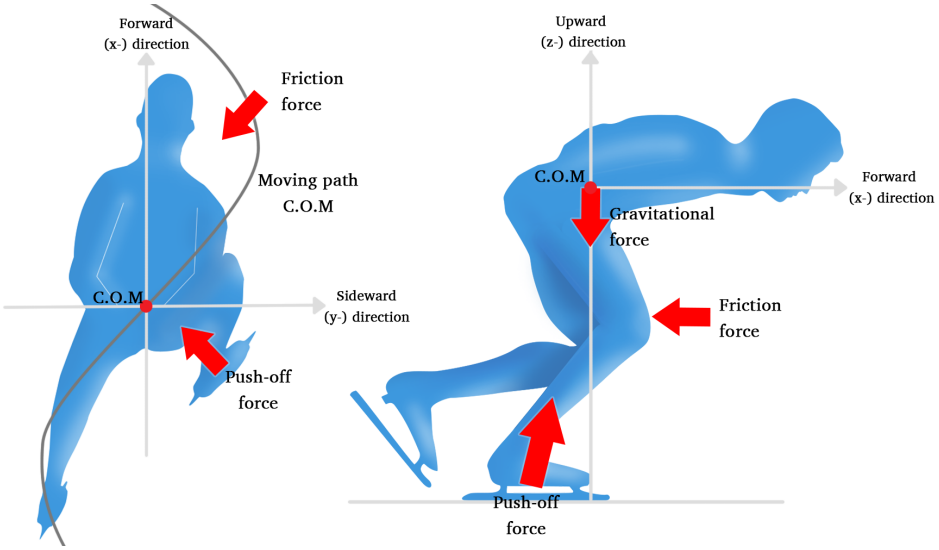

Figure A.1: Top view (left) and side view (right) of the forces working on the speed skater together with the orientation and definitions of the axes.

Next to push-off power and friction power, could the power also be generated by the transfer of power due to steering of the skates or falling motion of the skater. The steering and falling motion of the speed skater are assumed to have a role in the change of power, but cannot be measured with this method. Therefore, these effects are neglected for the three-dimensional power balance model.

The friction power exists of air and ice friction and is based on the frontal area of the skater (Van Ingen Schenau et al. 1985). The sideways push-off technique causes the frontal area of the skate to be not aligned with the forward direction. The air friction is therefore present in both forward and sideward direction. The breakdown of the friction in each direction is described by θ, the angle between forward and sideward velocity of the skater. The friction in the upward direction is assumed to be low, and is therefore neglected. The air friction is modeled with a dependency on velocity and requires estimation of the air friction coefficient (k_1). The ice friction is modeled as coulomb friction, which requires estimation of the ice friction coefficient (μ, De Koning et al. 1992).

$$\begin{aligned} F_{fr} &= k_1\left(v_x^2 + v_y^2\right) + \mu mg \\ P_{fr_x} &= F_{fr} \cdot \cos(\theta) \cdot v_x \\ P_{fr_y} &= F_{fr} \cdot \sin(\theta) \cdot v_y \end{aligned} \tag{A.3}$$

The power balance model is made massless by dividing the equations by the mass. This enables the mechanical power of different skaters with different masses to be compared. The mechanical power is defined in Watt per kilogram (Wkg^{-1}). In concussion, the three-dimensional power balance model is defined as:

$$\begin{aligned} P_x &= v_x a_x + \left(\frac{k_1}{m}\left(v_x^2 + v_y^2\right) + \mu g\right) \cdot \cos(\theta) \cdot v_x \\ P_y &= v_y a_y + \left(\frac{k_1}{m}\left(v_x^2 + v_y^2\right) + \mu g\right) \cdot \sin(\theta) \cdot v_y \\ P_z &= v_z a_z + g \cdot v_z \end{aligned} \tag{A.4}$$

Friction coefficients
The air friction coefficients can be obtained by wind tunnel experiments (Van Ingen Schenau 1982) or gliding experiments (Fintelman 2011). Wind tunnel experiments result in accurate estimations of the air friction coefficients and are subject specific, but are time intensive and complex to execute. The gliding experiment is a relative simple experiment, which produces a rough estimation of both air and ice friction coefficients. Most speed skating research uses the general air friction estimation derived with wind tunnel experiments by Van Ingen Schenau, which is reported by De Koning et al. (2000) as:

$$\begin{aligned} k_1 =& 0.0205 l m^{\frac{1}{3}} (0.798 + 0.0132\theta_1)(0.167 + 0.00757\theta_0) \\ & (4.028 - 0.809 ln(v) - 0.189v + 0.00866v^2)\rho_0 e^{-0.000125h} \end{aligned} \tag{A.5}$$

where l is the body length, m is the body mass, θ_1 is the angle of the trunk with the horizontal, θ_0 is the knee joint angle, v is the velocity, $ln(v)$ is the natural logarithm of the velocity, ρ_0 is the air density at sea level and h is the altitude above sea. To fit the air friction coefficient to the skater, it is required to measure the trunk and knee angle during the experiment. In most cases is the average trunk angle used for estimation of the air friction.

The gliding experiment performed by Fintelman estimates both air and ice friction coefficients by the deceleration of a skater. The skater glides with a constant posture in a straight line over the ice and decelerates due to air and ice friction working against the speed skater. The ratio between ice and air friction was estimated at 80% and the friction coefficients were assumed independent of the posture.

The ice friction coefficients can be found using force measurement skates (De Koning et al. 1992) or, as previously described, with the gliding experiment (Fintelman 2011).

In this study are the air and ice friction estimated with the gliding experiment. This friction estimation requires less computation with respect to the wind tunnel experiment and it gives subject and location specific air and ice friction coefficient.

A.1.3 Devices

The three-dimensional power balance model requires measurements of velocity and acceleration during the experiment, and estimations of the air and ice friction coefficients for the friction force. These friction coefficients require measurements of the acceleration. This chapter describes and selects the possible measurement devices for measuring the acceleration and velocity.

Previously Used Measurement Devices
The literature thesis of Van der Kruk (2013a) analyzed the possible three-dimensional positioning measurement systems during speed skating and used the iGPS system of Nikon as primary measurement device in her graduation study (Van der Kruk 2013b). Her study suffered from data gaps and did not reach her expected accuracy. In addition, the LPM (Local Positioning Measurement, inmotio) system was used as a secondary position measurement system in this study. Van Der Kruk concluded that the LPM system is only accurate on the average velocity for a longer period. In conclusion, Van Der Kruk stated improvements to one, or both, systems to increase the accuracy during ice-skating experiment.

There are two other options to measure the velocity and acceleration during speed skating: with an accelerometer or by video analysis. Video analysis is not considered for this thesis, because it is assumed to require a lot of post-processing and expensive camera's with a high frame rate. Van der Kruk (2013b) and Fintelman (2011) used the Xsens MTi (Xsens) device for orientation measurements, but this device can also be used to measure solely acceleration. However, the acceleration measurements would also require orientation measurements, because the sensor cannot be fixed in the wanted track orientation: the sensor would be placed on the skaters back, which is constantly moving with respect to the track orientation. The study of Van Der Kruk stated that the orientation measurements are very accurate during ice skating measurements, and require to be improved. The accelerations can be measured very accurate with this device, but the derivation of the velocity with an accelerometer is inaccurate over a longer period of time. Integration errors will increase in time due to measurement errors in the devices.

Device Selection
Both LPM position and Xsens LPM measurement system were selected to measure the acceleration and velocity. Using only one of those measurement systems would not be beneficial for the accuracy of both velocity and acceleration measurements. The Xsens MTI device was used for acceleration measurements, and data from the Xsens MTi and LPM devices were fused to improve the known low accuracy and limitations of the systems for velocity measurements. The LPM position measurement system was selected over the iGPS system, because the data gaps will probably be present. The time limit on the study excluded the option to improve or experiment with this measurement systems. The system did also require a clear ice rink and placement of minimal 10 transponders near the ice track. The LPM system does not fit all the requirements for the thesis: the LPM system lacks the upward position measurement dimension and is inaccurate with position measurements during high sampling frequencies. However, the LPM system a stable system and is daily used as velocity measurement system in ice-rink Thialf (Heerenveen, The Nederlands).

There are multiple options to combine the LPM position and Xsens MTi acceleration data for the velocity. Two options were investigated. The first option is to fuse the data of both sensors with a Kalman-filter to estimate the true velocity. The Kalman-filter can correct the velocity measurement on basis of both measurements with their corresponding expected error. Implementing and testing the Kalman-filter is complex and requires a lot of time. The second option is to also fuse the data of both sensors to estimate the true velocity, but only uses the strong points of both measurement systems. The velocity estimation with the LPM system is most accurate if the average position over a longer time is used. The velocity estimation with the Xsens MTi sensor is most accurate on short periods of time. The short periods of time reduce the absolute velocity measurements to relative velocity measurements; the initial velocity is unknown. The relative velocity was calculated with integration of the acceleration and adding the average absolute velocity calculated by differentiating the position data. The second option was selected to calculate of the velocity. The data is assumed to give a relative accurate velocity, without creating a relative complex Kalman-filter.

A.2 Energy Expenditure Measurement

A.2.1 Methods

Energy expenditure in sports can be estimated by two approaches: by *indirect calorimetry* (e.g. oxygen uptake) or by *non-calorimetric* (e.g. heat rate, Levine 2007). Van Ingen Schenau et al. (1983), De Boer et al. (1987a), Houdijk et al. (2000a) and De Koning et al. (2005) measured the oxygen uptake during speed skating and Van Ingen Schenau et al. (1983), De Boer et al. (1987b) and Houdijk et al. (2000a) the heart rate during speed skating.

There are limitations on the estimation of the energy expenditure by oxygen uptake and heart rate: there is only a linear relation between the oxygen uptake and energy expenditure during a submaximal exercise (Keim et al. 2004). In addition, the heart rate is only linearly related to oxygen uptake for dynamic activities involving large muscle groups (Crouter et al. 2004). Therefore, it is required to measure the oxygen uptake or energy expenditure if the speed skater is skating of already a couple of minutes: the skater will then have reached the steady state. Farringdon and Wolf (2006) noted that the heart rate relation is only adequate by comparing the heart rate under the same controlled conditions. The controlled conditions are, among others, the submaximal exercise level, environmental factors, stress factors and hydration levels. It takes some amount of time to stabilize the energy expenditure and to only see the effect of the constant push-off exercise. The energy expenditure will be used to compare the different push-off techniques and other effects on the energy expenditure required to be limited to only measure the true effect of the different push-off effect. Heart rate measurements do not measure the absolute energy expenditure, but only the relative energy expenditure. It can only be used to describe the difference in energy expenditure between subjects.

Even with the possible higher accuracy and absolute energy expenditure measurements with the oxyen uptake is the heart rate measurement selected over the oxygen uptake measurement to estimate the energy expenditure. Heart rate measurements devices are standard used by almost all speed skaters and assumed simpler in setup and usage than oxygen uptake measurements.

A.2.2 Devices

Each logging heart rate device can be selected to estimate the energy expenditure. A polar chest band (version unknown) is selected, because this polar chest band is part of the LPM system. The polar chest band is automatically synchronized and stored in the LPM system.

APPENDIX B

Measurement Devices

This section explains the settings, post-processing and placement of Xsens MTi device, LPM device, Polar device, camera and their peripheral devices.

B.1 Xsens MTi and AntiLog

The Xsens MTI (Xsens MTi-28A53G35, Xsens, Figure B.1) is an inertial measurement unit (IMU) and exists of 3 accelerometers, 3 gyroscopes and 3 magnetometers. An advanced Kalman-filter uses these internal sensors to measure the orientation with respect to a fixed global reference frame. Both the acceleration and orientation measurements were used for the mechanical power measurements. The sample frequency was set at 200Hz, the orientation data was represented in an orientation matrix and the Xsens Kalman Filter (XKF) "Machine" is used. See Figure B.1 for all settings of the Xsens MTi device.
Three Xsens Kalman Filters (Machine, Human and Human Large Accelerations) were tested on their performance during static and dynamic conditions in an indoor ice-rink (De Uithof, Den Haag, The Netherlands). None of the filters did increase the orientation accuracy to an acceptable level, but the "Machine" Kalman Filter was expected to perform the best. The test is not documented, because not enough measurements were performed to statistical select the best filter and the results were not assumed very accurate. No field mapping for the surrounding external devices was performed and the device was not as solid attached as with the experiment used in this study.

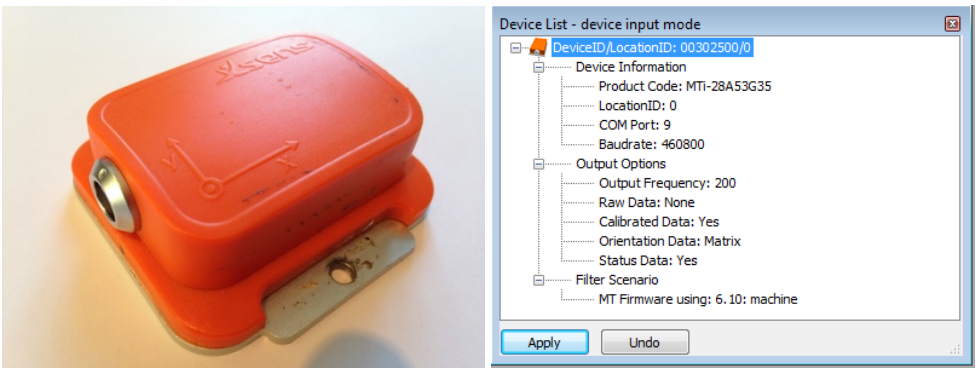

Figure B.1: The Xsens MTi device (left) and settings of the Xsens MTi device (right)

The analog data of the Xsens MTi device was stored in binary format on an external data logger (AntiLog v5.1, AntiCyclone Systems) and was powered with an external battery (4xAA). The Xsens MTi, data logger and battery were positioned on a belt (Figure B.2), which is placed on the speed skaters back. Field mapping was conducted with the Xsens and peripheral devices on the belt to reduce the effects of nearby devices and metals.
The local acceleration, in three dimensions, and orientation of the device, with respect to the global reference frame, were extracted with a specially written Matlab code, which is based on the Xsens MTi low-level communication protocol documentation (Xsens Technologies 2010). The orientation

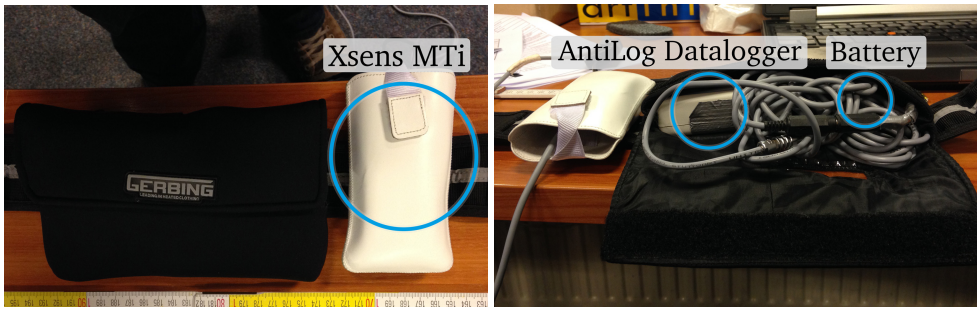

Figure B.2: Placement of the Xsens MTi, data logger and battery on a belt.

matrix is converted from the orientation matrix notation to a XYZ-Euler notation.

The measured local orientation of the accelerations was not equal to the track orientation of the power balance model (Figure B.3). Due to the movement of the skater, the orientation of the device changed frequently with respect to the track orientation. The device measured the local orientation with respect to the global orientation and not with respect to the track orientation. The global orientation was defined as the x-axis aligned with the magnetic north, the z-axis aligned with the gravitation force, and the y-axis perpendicular to the x- and z-axes. The difference between the track and global orientation is a rotation around the z-axis. The required rotation around the z-axis was calculated from the average rotation around the z-axis. The average rotation around the z-axis describes the forward (x) track orientation of the skater (Figure B.3).

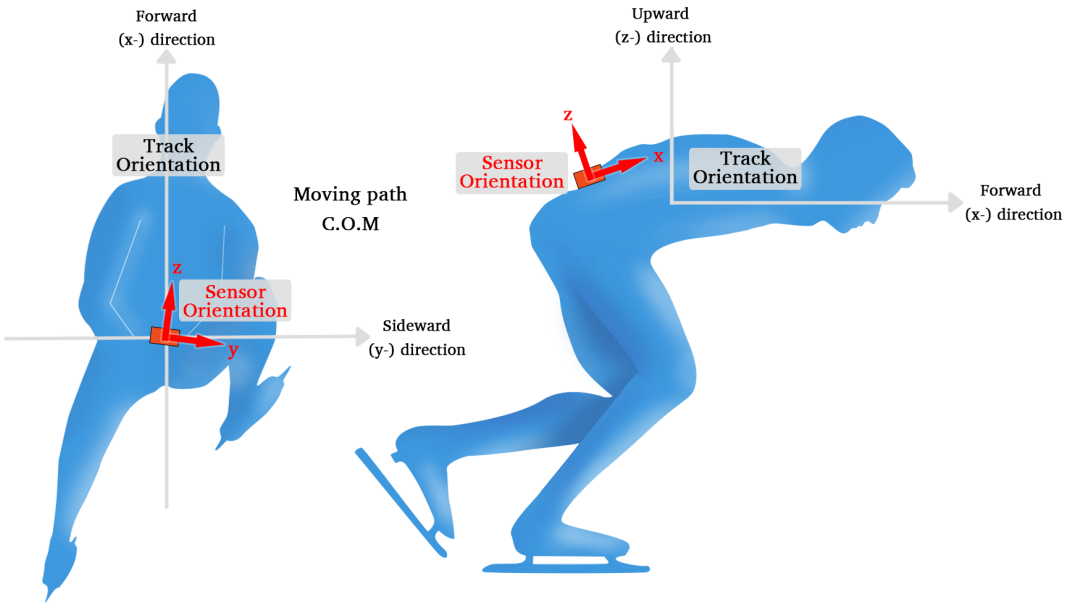

Figure B.3: Orientation of the Xsens on the back of the skater (Sensor Orientation) with respect to the track orientation.

The global orientation measurements in an indoor ice-rink were assumed not accurate enough to use the transferred acceleration directly for power calculations. The orientation was corrected with an optimization method (Appendix D).

B.2 LPM

The stationary and moving LPM devices (Inmotio) were wirelessly stored on an external computer with LPM software. The LPM system consists of a position sensor and heart rate sensor.

Position sensor
The moving LPM device was placed with a vest, included by LPM, on the shoulders of the speed skater (Figure B.4 (left)). The stationary LPM device was placed on a camera tripod near the ice (Figure B.4 (right)). The sample frequency varied between 250 and 500 Hz, depending on the number of devices in use.

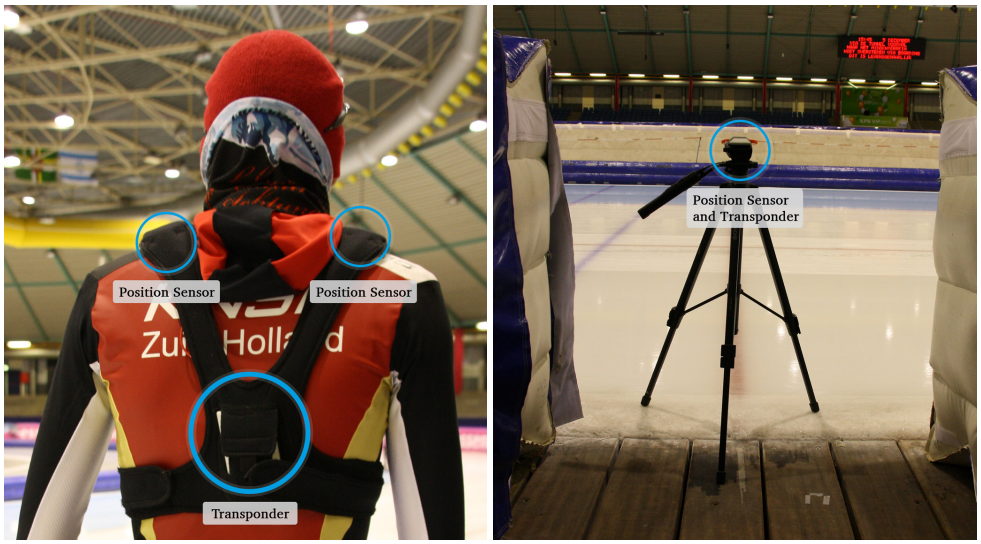

Figure B.4: The moving LPM device in a vest on the skaters back (left) and the stationary LPM device on a tripod in the ice (right).

Polar Heart Rate Band
Polar heart rate chest belt (model unknown, Polar) registered the heart rate of the speed skater. The device was placed directly onto the skin of the subjects' chest. The polar device was wirelessly connected to the LPM receiver on the speed skaters back. The wireless connection ensured synchronization and storage of the heart rate on the LPM computer.

The position with respect to a relative position in the middle of the ice-rink and heart rate were exported from the stored data on the LPM computer. The position and heart rate was exported with a sample frequency of 200Hz and filtered with a linear filter. The position data is futher filtered with self-written Matlab software, which included a running mean of 5 samples. The velocity is calculated by differentiating the position and applying a running mean of 2 samples to reduce measurement errors.

B.3 Stationary Camera

The stationary camera (Sony) was only used for synchronization of the LPM and Xsens MTi devices. The device was placed on a tripod, in line with the placement of the stationary LPM sensor near the ice (Figure B.5).

The data of the stationary camera was saved as MTS file (AVCHD format, MPEG-4 AVC/H.264 video code) at 1080p and with a frame rate of 25 frames per second. The video was converted to an AVI file (MPEG-4 Xvid codec).

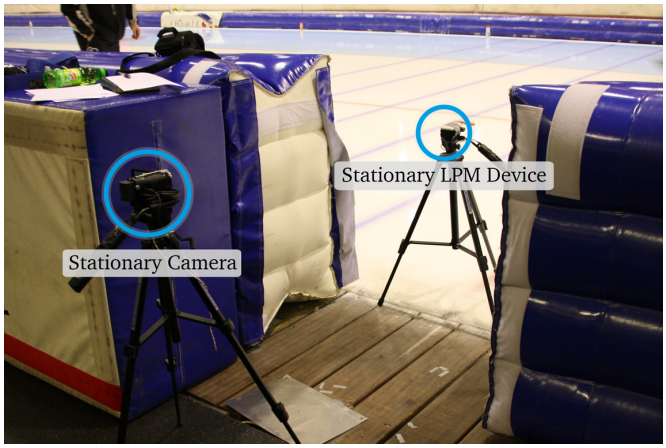

Figure B.5: Placement of the stationary camera and stationary LPM sensor for the synchronization protocol.

APPENDIX C

Air and Ice Friction Estimation

This appendix describes the method to estimate the air and ice friction coefficients of the skaters with an gliding experiment. It is essential to estimate the air and ice friction forces for the calculation of the forward and sideward human power components. The total friction force exists of air (F_{air}) and ice friction (F_{ice}) forces:

$$P_{fr} = F_{fr}v = F_{air}v + F_{ice}v \tag{C.1}$$

Air and ice friction forces during speed skating push-offs can be estimated with air (k_1) and ice friction (μ) coefficients (Equation (C.2), Van Ingen Schenau 1982, De Koning et al. 1991b). These coefficients were calculated with a slightly changed gliding experiment described by Fintelman 2011).

$$P_{fr} = \left(k_1 v^2\right) v + (\mu m g)\, v \tag{C.2}$$

C.1 Gliding Experiment Method

The gliding experiment was performed directly after the last lap of the power distribution experiment. The skaters were instructed to glide with both skates on the ice during one straight part of the track. They glided on a straight-line parallel on the ice-track in about the same, but static, posture as during skating. The air and ice friction forces were calculated on the average deceleration of the speed skater and the air-ice distribution ratio β (Equation (C.3)). The average deceleration times mass is equal to the friction force.

$$\begin{aligned} F_{fr} &= ma_x \\ F_{air} &= \beta F_{fr} = k_1 v^2 \\ F_{ice} &= (1-\beta) F_{fr} = mgv \end{aligned} \tag{C.3}$$

The air friction coefficient during skating is dependent on the trunk angle, knee angle and velocity (Equation (A.5)). The trunk and knee angles are assumed equal to the average angles during skating. The air friction coefficient was corrected by the average gliding velocity (v_g) to match the skating velocity of $11.0 ms^{-1}$ and $9.7 ms^{-1}$ (v_{cor}, Equation (C.4)).

$$\begin{aligned} H(v) &= 4.028 - 0.809 ln(v) - 0.189v + 0.00866v^2 \\ k_1 &= \frac{\beta F_{fr}}{v_g^2 H(v_g)} H(v_{cor}) \end{aligned} \tag{C.4}$$

The air and friction ratio β describes the friction force losses due to air and ice friction ratio with respect to the lap times. Fintelman used a ratio of 0.8 (De Koning et al. 1991b), which is the relation between air and ice friction during speed skating at $11 ms^{-1}$ (Gemser et al. 1999). For this experiment

is the ratio set at 0.95. The ice friction during only gliding is assumed lower in comparison with speed skating. Steering and push-off of the skates during skating increases the friction forces (Houdijk et al. 2001). The main contribution of friction during gliding is due to the air friction forces.

The average acceleration during the gliding experiment was calculated by fitting a polynomial through the forward velocity. The position data from the LPM sensor was selected for calculating the velocity. The data was post-processed with the same method as for the power distribution experiment. The velocity trend line was defined as a first order polynomial (Equation (C.5), Figure C.1). Only moments on which the skaters sideward velocity was minimal were used to fit the polynomials.

$$v_x = a_x t + v_{x_o} \tag{C.5}$$

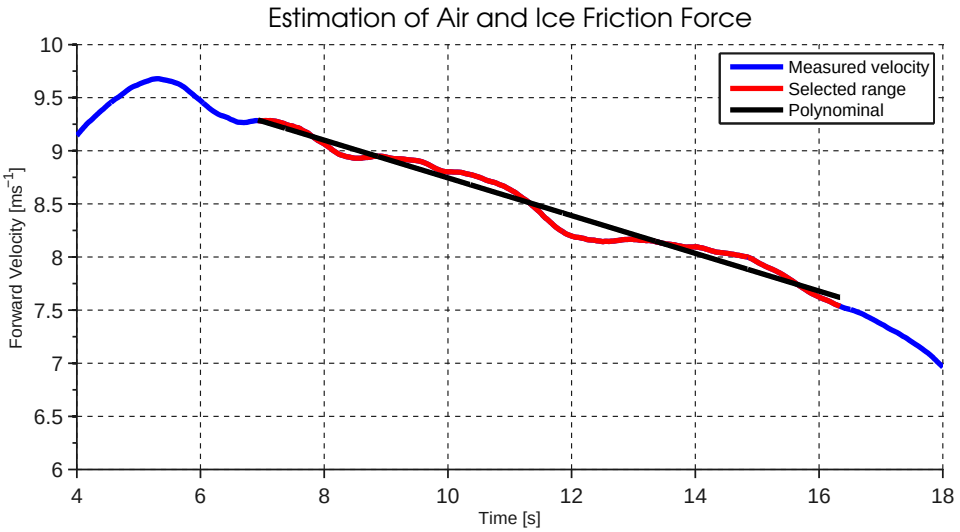

Figure C.1: Polynomial for estimation of the average deceleration of the speed skater during gliding experiment.

C.2 Results

Seven skaters have performed three gliding trials, and the results of the air and ice friction, together with the average air and ice friction of the three trials, are given in Figure C.2). The average air and ice friction coefficients were $0.1207 \pm 0.0146 Ns^{-2}m^{-2}$ and 0.0009 ± 0.0001, respectively.

C.3 Discussion

Air Friction Coefficient
The resulted average air friction coefficient ($0.1207 \pm 0.0146 Ns^{-2}m^{-2}$) is lower than reported by Fintelman ($0.1615 - 0.1716 Ns^{-2}m^{-2}$), which are according to Fintelman the same order of magnitude as measured by De Koning et al. (1992) and Van Ingen Schenau (1982). The used method to calculate the friction forces was different than used by Fintelman. Fintelman did not compensate for the gliding velocity and did have a higher air-ice friction ratio β. The air friction coefficient does not match Fintelman's values, when the same calculation method was used ($0.1239 \pm 0.0111 Ns^{-2}m^{-2}$).

The air friction coefficient calculated with the air friction model described by De Koning (Equation (A.5)), for average mass and length, velocities of $11 ms^{-1}$ and trunk and knee angles of respectively 110° and 20° becomes $0.1618 Ns^{-2}m^{-2}$. This air friction coefficient is also 25% higher reported

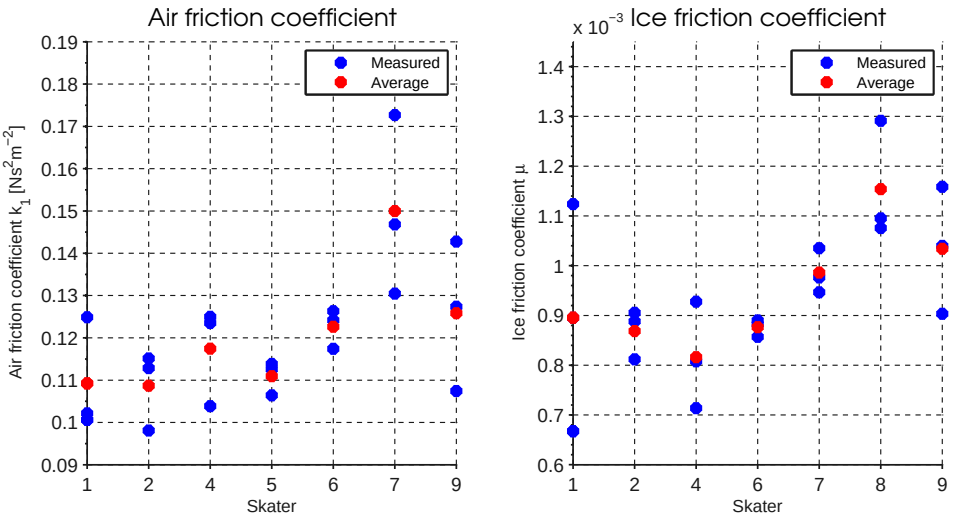

Figure C.2: Air and Ice Friction results of the gliding experiment.

in this study and do match the value of Fintelman. The lower reported air friction could be the result of other skaters moving past the gliding skater. Van Ingen Schenau (1982) did analyze the effect of shielding a skater. The air friction coefficient decrease 16% to 23% if the skater is respectively 2 or 1 meter directly in front of the skater. The gliding experiment was not directly filmed and there is no definitive prove of skaters moving directly in front of the speed skater, but there were moving other skaters alongside and in front of the gliding subject. Another option of the lower air friction is the posture of the skater. The knee and trunk angles of the skater were not measured. A trunk and knee angle of respectively 10° and 100°, the lowest common values reported values (Gemser et al. 1999), decreases the air friction coefficient by 14%. The exact reason for the lower observed air friction coefficient cannot be stated, but it is most likely a combination of passing skaters and different (lower) knee and trunk angles.

Friction Coefficient
The resulted ice friction coefficients (0.0009 ± 0.0001) are lower than reported by the gliding experiment of Fintelman ($0.0025 - 0.0041$), De Boer et al. 1987b, 0.006) and De Koning et al. 1992, 0.005). The reason for the lower ice friction is the higher air-ice friction ratio β. The lower air friction was also expected, since the speed skater was only gliding over the ice, and not pushing off.

C.4 Conclusion

This experiment could not conclude that the friction coefficients were correct or that the friction forces in literature are. The gliding experiment measured the air friction of the skater, with different postures, inside the ice-rink under the actual skating conditions and the same skater. The data in literature used the air friction of the skater, with an average skating posture and not the same skater, inside a wind tunnel under experimental skating conditions. Both measurements methods are not ideal for measurement of subject and location specific air and ice friction forces during speed skating.

APPENDIX D

Optimization of Orientation

The global orientation measurements in an indoor ice-rink were assumed not accurate enough to use the transferred acceleration directly for power calculations. The orientation was corrected with an optimization method. This chapter describes the observed orientation errors and the optimization method.

D.1 Global Orientation Errors

Z-axis Offset
The errors in the global orientation measurements were visible in the rotation around the z-axis. The offset between the track and global z-axis should be constant for each of the two straight parts of an ice-rink, but this was not observed (Figure D.1). Each data is created by a single skater with a certain technique and exists of 11 straight parts, which exist each of 1 to 3 stroke-cycles. The orientation offset between the track and global orientation was calculated for each stroke-cycle. The result in Figure 12.1 represents the average error of all stroke-cycles combined and the standard deviation of the spread within the stroke-cycles. The average offset between the track and global z-axis of the 21 datasets combined is $27.1 \pm 11.0°$. The spread of the offset angle in Figure D.1 states the inaccuracy of the assumed constant offset angle. The high spread of each dataset does indicate that the offset is not a constant offset for each dataset, but is a random error in the orientation.

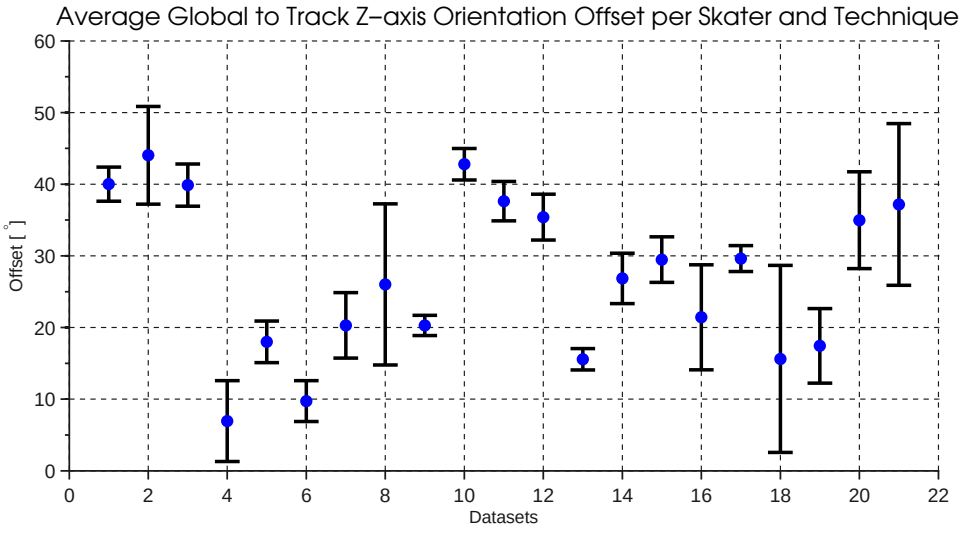

Figure D.1: Average global to track z-axis orientation offset per skater and technique.

Accelerations
The effects of the inaccurate global orientation were also visible in the accelerations. The push-off of the speed skater was assumed symmetrical for each push-off leg. The sideward acceleration in the track orientation required therefore also to be symmetrical during one stroke-cycle, but this was

not observed (Figure D.2). The peak value of each push-off was not symmetrical; the first push-off generated a maximum acceleration of $12.9ms^{-2}$, while the push-off with the other leg was only $-9.5ms^{-2}$. This asymmetry was noticeable in each stroke-cycle. It was assumed that this effect is the result of the errors in the global orientation measurements and not in the acceleration measurement. A simple static experiment (not included in this thesis) showed that the acceleration in each direction was equal to the expected gravitational force.

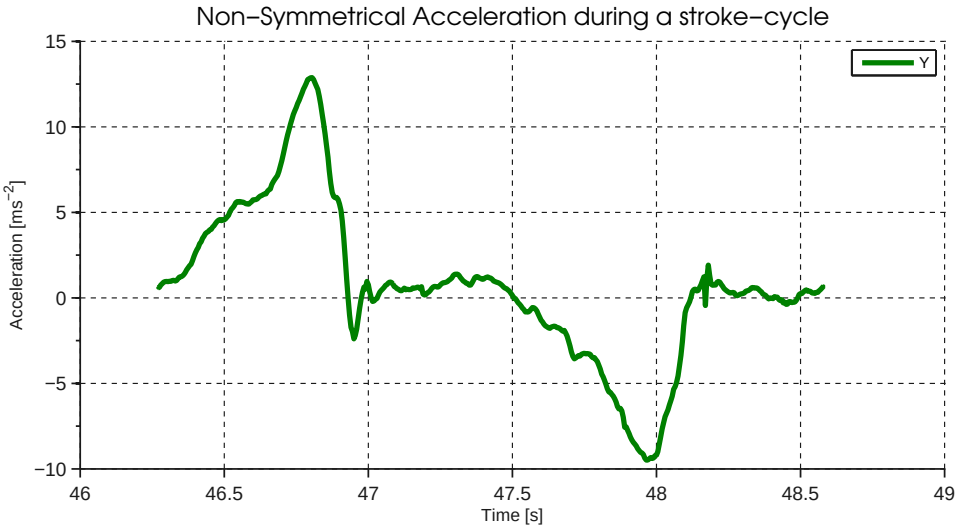

Figure D.2: Non-symmetrical acceleration in sideward direction during one stroke-cycle.

Optimization

The observed spread in the z-axis offset suggests a random error in the orientation, and no constant error for each stroke-cycle or dataset. The random orientation error cannot be solved for each sample, because the real result is unknown. The error was therefore treated as a constant offset error over time. The shortest constant error will result in the best representation of the random error. The stroke-cycle was selected as the shortest time period. The average forward and sideward acceleration, measured with the Xsens device, required to match the average forward and sideward acceleration measured with the LPM device. The average upward acceleration was set equal to zero: the upward position of the skater is at the start and and of a stroke-cycle in the same position.

The simulated annealing optimization function ($simulannealbndm$, Matlab) was selected to find the optimal orientation offset at which the average accelerations in all directions matches the LPM measurements in forward and sideward direction and the assumed zero acceleration in upward direction. The goal of the optimization was to reduce the error between these accelerations. The error function expresses the error in each direction evenly. The average forward and upward error exists of the combined difference in average acceleration for the left and right push-off and the whole stroke-cycle. The left push-off was defined as the first half of the stroke-cycle, the right push-off as the second. These three sections were chosen, because otherwise the optimal orientation could represent very asymmetrical left and right leg push-offs. With this error functions, only symmetrical push-off were found, which was expected. The error function in the sideward acceleration existed only of the difference in average acceleration of the whole stroke-cycle, since the acceleration of both push-offs legs was not symmetrical in the sideward direction.

Simulated annealing is preferred over the grid or gradient search, which could result in local minima instead of the global minima solution. This optimization algorithm uses the gradient search to find the minima, but skips at random intervals forward or backwards to see if the error is lower a on another position. This reduces the changes to 'get stuck' in a local minimum instead of a global minimum. The optimization was constraint to find the global orientation within 10°, 20° and 30° lower or higher than the measured value in the x-, y- and z-axis respectively.

The main drawback observed with the simulated annealing function is the random skip to search for other minima's. Multiple optimizations of the same skater have resulted in different outcome in, for example, the forward power component. Differences up to $0.2Wkg^{-1}$ in the average forward power component of all skates have been observed.

Figure D.3 shows the result of the optimization procedure. The dotted lines describes the acceleration in each direction by only using the local to track orientation transformation. The solid lines describe the acceleration in each direction by optimizing the orientation. The optimized acceleration in the sideward y-direction is more symmetrical than the track acceleration. The x, y, and z-angles in this example are given an offset of $-2.8°$, $8.8°$, $-19.9°$ respectively.

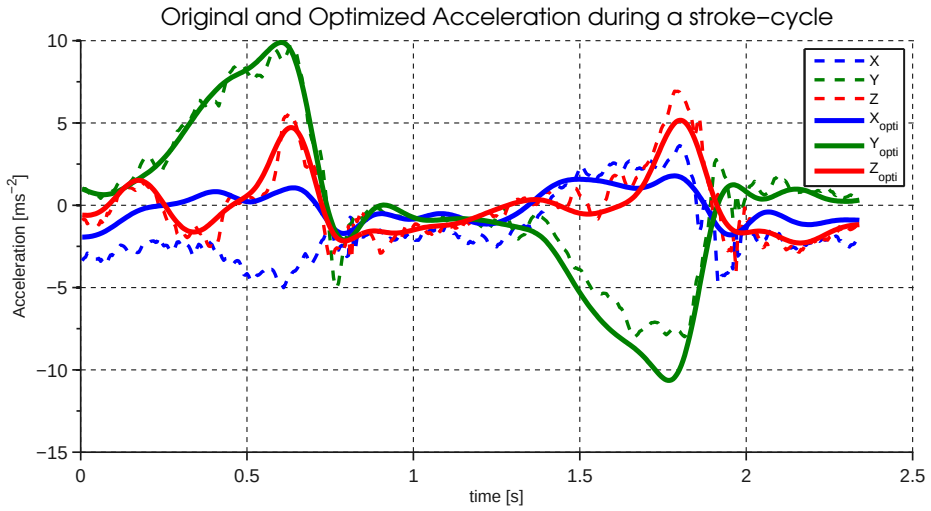

Figure D.3: Result of the optimization procedure for the acceleration during a stroke-cycle.

The optimization offset of all stroke-cycles of one skater with one technique is given in Figure D.4 and three stroke-cycles per straight are represented. The offset of each angle did not differ very much. There is somewhat of a pattern present per straight. Three succeeding stroke-cycles on one straight describe in most cases a decrease in the offset angle for the rotation around x and y. The spread of the optimization angles describe a random error and not a constant offset in the angles.

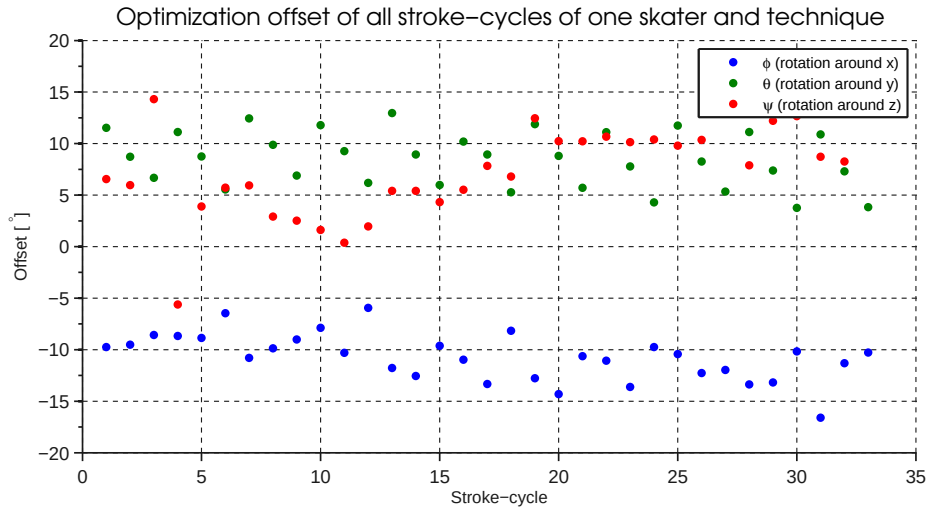

Figure D.4: Optimization offset of all stroke-cycles on one skater and technique.

APPENDIX E

Synchronization

The LPM and Xsens MTi data was synchronized by observing both devices with a stationary camera. Each dataset recorded the three push-off techniques of each skater. Ticks were applied to the Xsens MTi sensor and visible on both the acceleration data as the camera. The camera also recorded the moment the speed skater (with LPM sensor) passed alongside the stationary LPM sensor. The recording of both LPM and Xsens devices on the camera is the time difference and used for synchronization.

There were 24 ticks per dataset applied on the Xsens MTi device; 3x6 ticks before each push-off technique and 1x6 ticks at the end of the last push-off technique. The ticks in the acceleration were found automatically with self-written Matlab software (Figure E.1, bottom right). The range in which the peaks occur did require to be selected manually (Figure E.1, top right). The ticks in the video were found manually by a frame-by-frame analysis using VirtualDub (version 1.10.4, Figure E.1, left). The time difference between the acceleration and video tick was calculated for each tick. The mean time difference for all ticks was the time difference between the Xsens MTi and video devices.

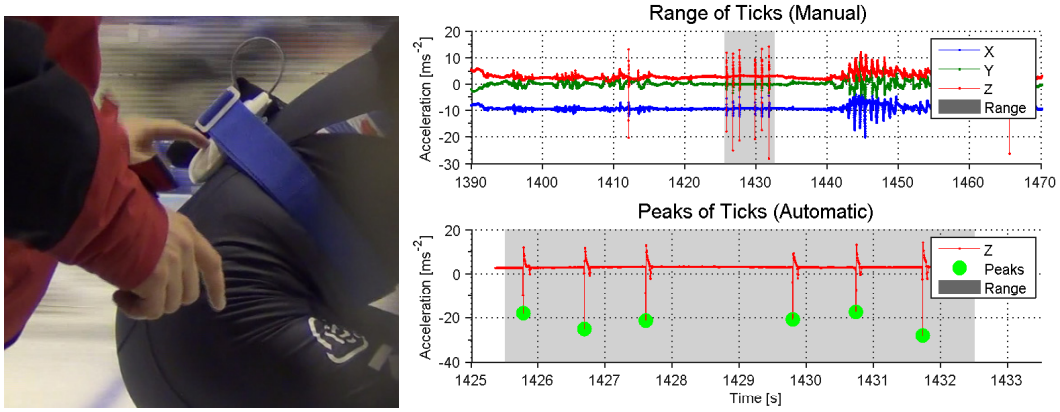

Figure E.1: Detection of ticks on the Xsens MTi device on the video (left) and on the acceleration (right). The manual selection of the peaks (top right) and the automatic selection of 3 peaks (bottom right).

The moment the speed skater passes the stationary camera was recorded with the position of the skater and the stationary camera. At this point, the position of the moving and stationary LPM device were equal (Figure E.2 right). A total of 3x6 synchronizations points were used each data set. The points in the video were found manually by a frame-by-frame analysis using VirtualDub (Figure E.2 left). The difference in time between the positions on the LPM sensor and frames was calculated for each point. The mean time difference for all ticks, was the time difference between the LPM and video devices.

Fine-tuning
The relative low sample frequency of the camera and high moving velocity made it difficult to notice the moving of the skater on the video images. Therefore, the synchronization was fine-tuned by finding the best fit in sideward velocity between the Xsens and LPM data. The not optimized sideward

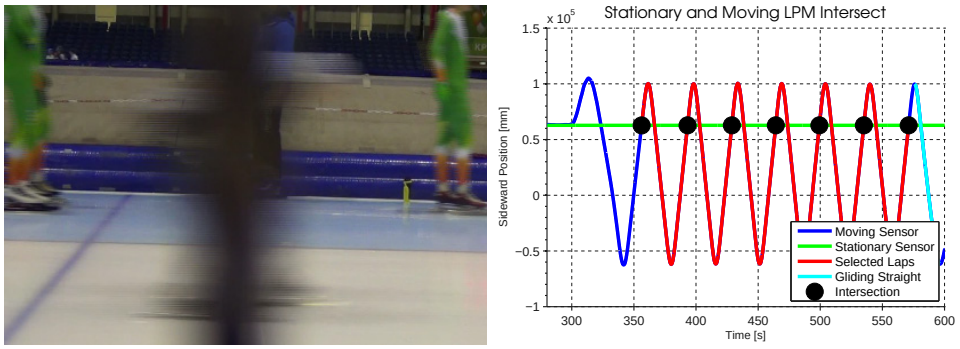

Figure E.2: Detection of the passing of stationary LPM sensor by the speed skater on the video (left) and on the position data of the skater (red line) and stationary position (green).

track acceleration was used to calculate the sideward velocity during a stroke-cycle. The sideward velocity was also calculated with the sideward position data. The best fit between these datasets was the fine-tuned time synchronization between the two devices. The average time synchronization of all stroke-cycles in a dataset was used for the final synchronization time.

APPENDIX F

Stroke-Cycle

F.1 Stroke-Cycle Selection

The stroke-cycles during the straight part of the track were selected for mechanical power measurements. The acceleration and velocity of all stroke-cycles of one skater with a certain technique were combined to create one stroke-cycle, which can represent the push-off technique of a specific skater with a certain technique. The averaging of all stroke-cycles of the skater reduces the human inconsistencies as well as measurement errors. The stroke-cycles were automatically selected with a self-written Matlab-script.

The position data of the LPM system was used to select the straight parts of the track and the peaks in acceleration to identify the push-off of each leg. Any point could be selected as the start of a push-off, because the speed skating movement is a repetitive cycle. The point before the large rise in the acceleration was chosen as the start of the stroke-cycle. This point is more or less also the start of the push-off phase (Figure F.1).

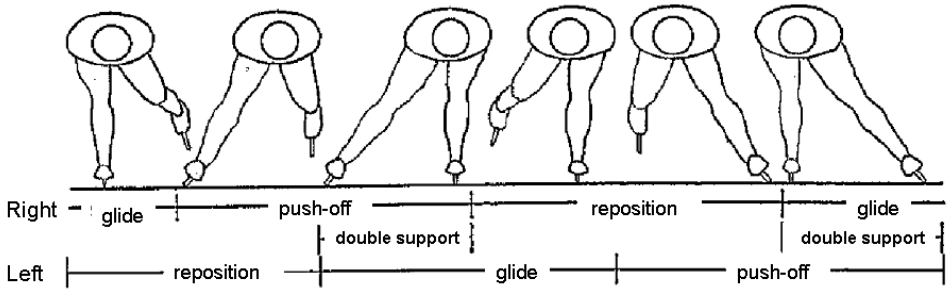

Figure F.1: Phases of a stroke: push-off phase, glide phase and reposition phase (Allinger and Van den Bogert 1997)

Figure F.2 is a screenshot of the stroke-cycle selection method. The data shows the position (red) and acceleration (blue) during one straight part of the track. The red dot indicates the different push-off cycle. Large oscillation were removed by averaging and applying a low pass filter on the data. This was preformed to select the start of the stroke-cycle correctly. The black dot is the start of the stroke-cycle. The data modification is only used for the selection of the start point, not for the calculation of the mechanical power. The gray area's show the range of each stroke-cycle during a straight part of the track. The script was optimized to only select the stroke-cycles, which were assumed selected correctly, and only describe a normal push-off pattern.

F.2 Representative Stroke-Cycle

Not all stroke-cycles were exactly similar, but they all described the same, but stretched, pattern in acceleration and velocity. The duration of the movement was eliminated by representing the stroke-cycles as a percentage of the stroke-cycle. This same processes was also performed by analysis

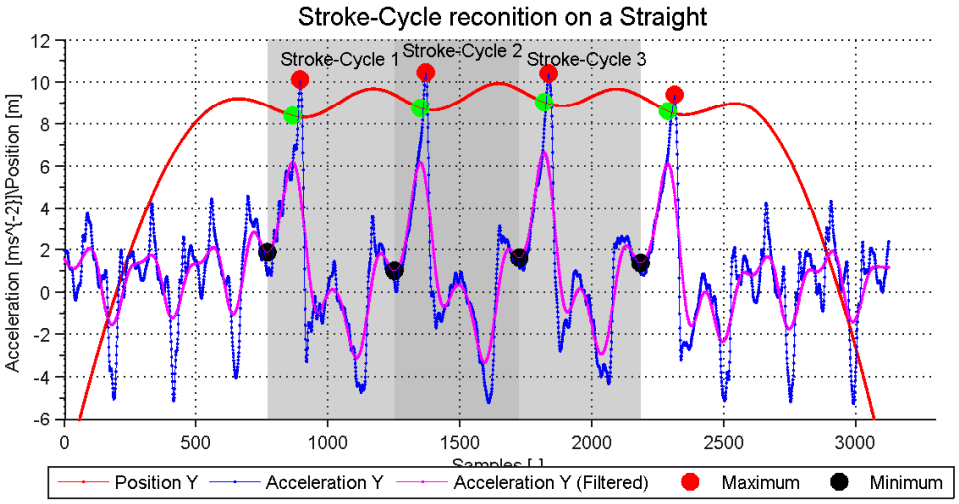

Figure F.2: Image off stroke-cycle selection

for the human gait: gait cycles. With this method, the important acceleration and velocity pattern of all stroke-cycles of a specific skater and technique were obtained.

Figure F.3 represents the acceleration of all stroke-cycles with one skater and one technique. The average acceleration was created by averaging all accelerations. This represents the representative acceleration of this specific skater and technique. The same averaging was also done for the velocity in the forward, sideward and upward direction. The mechanical power in each direction was calculated on basis of this representative velocity and acceleration.

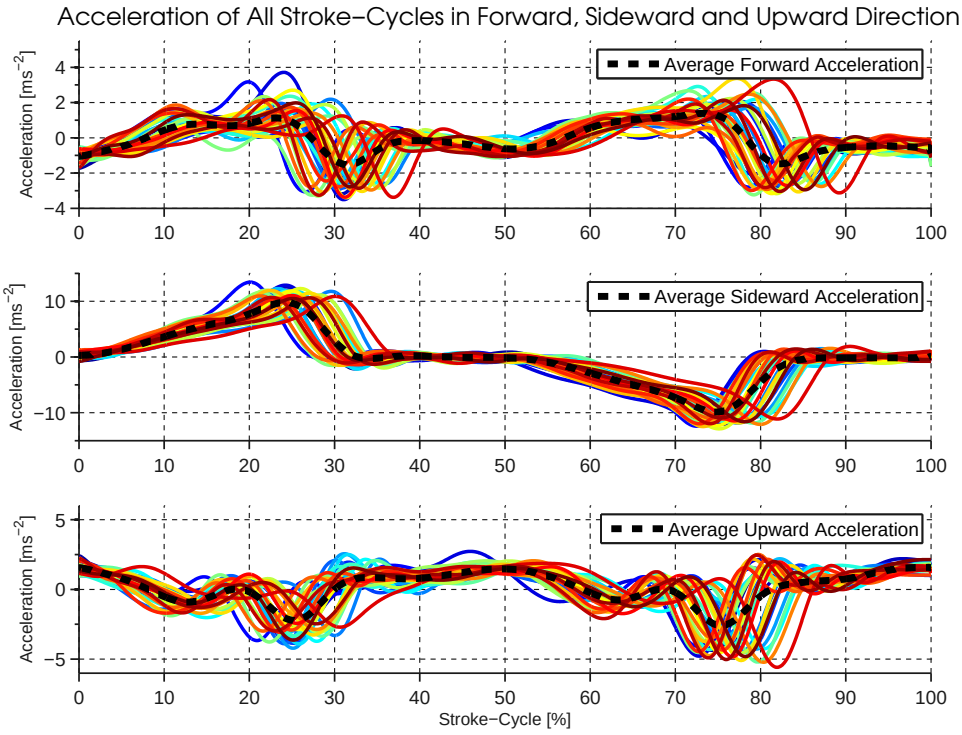

Figure F.3: Acceleration of all stroke-cycles in forward, sideward and upward direction. Data is obtained from all recognized stroke-cycles of one skater, with one push-off technque.

APPENDIX G

Power During a Stroke-Cycle

This thesis only focused on the average mechanical power of the representative stroke-cycles. However, the mechanical power within a stroke-cycle could also be analyzed with this method. This chapter investigates the mechanical power during a stroke-cycle. In addition, this chapter discusses the velocity and acceleration during a stroke-cycle. In the first section is only the self-chosen push-off technique reported and discussed. Afterwards, the difference of the small, self-chosen and wide are discussed.

G.1 Self-Chosen Push-off Technique

G.1.1 Results

Power
The forward, sideward and upward mechanical power components were approximately equal for the push-off of the left and right leg during a stroke-cycle. This could be observed in the two repeated patterns during a stroke-cycle (Figure G.1). This effect was also expected, since the two push-off movements of the legs were assumed symmetrical.

Two peaks in the forward power component were most noticeable during the push-off. The forward power component has the largest amplitude of the all power components and was, during a stroke-cycle, both positive and negative. In contrast, the sideward and upward power components were always positive. The forward power component increased after 0% and 50% of the stroke-cycle and keeps increasing until 25% and 75% of the stroke-cycle. Afterwards, the forward power component decreased rapidly.

The twice-repeated pattern in the sideward power component existed of two peaks. The sideward power component increased at approximately the same point as the forward power component and decreased somewhat after the forward power component decreased. The pattern was repeated after the sideward power stayed around zero for some time. The sideward power was in magnitude lower than the forward power.

The twice-repeated pattern in the upward power component increased around the same point as the forward power component increased and was zero when the forward power component was maximal. The magnitude of the upward velocity was in the same range as the sideward power. The first part of the upward power component was different from the rest (See Figure 15.4 for a detailed view). The power was in the first part twice as low as the other parts.

The total mechanical power described almost the same patterns as the forward power and has the same characteristics as the forward power component.

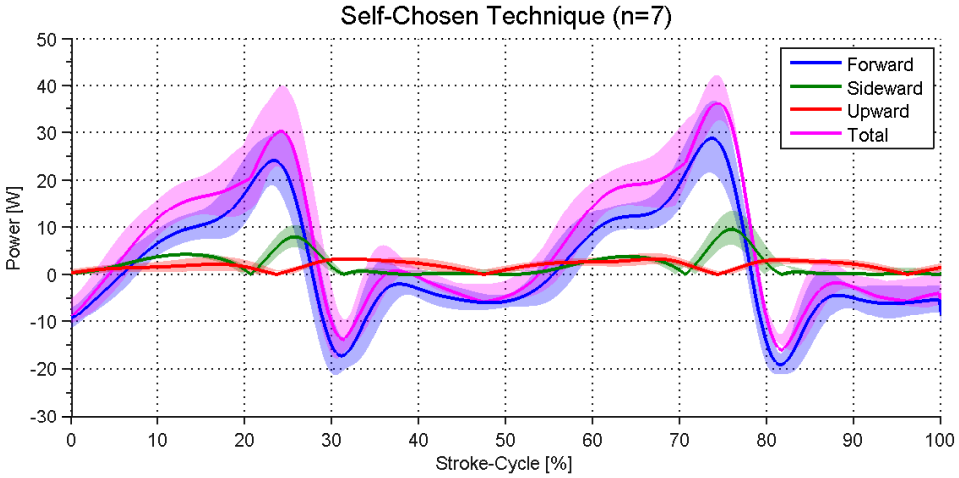

Figure G.1: Power during a stroke-cycle of the self-chosen push-off technique, where the colored surface is the standard deviation of the corresponding power components.

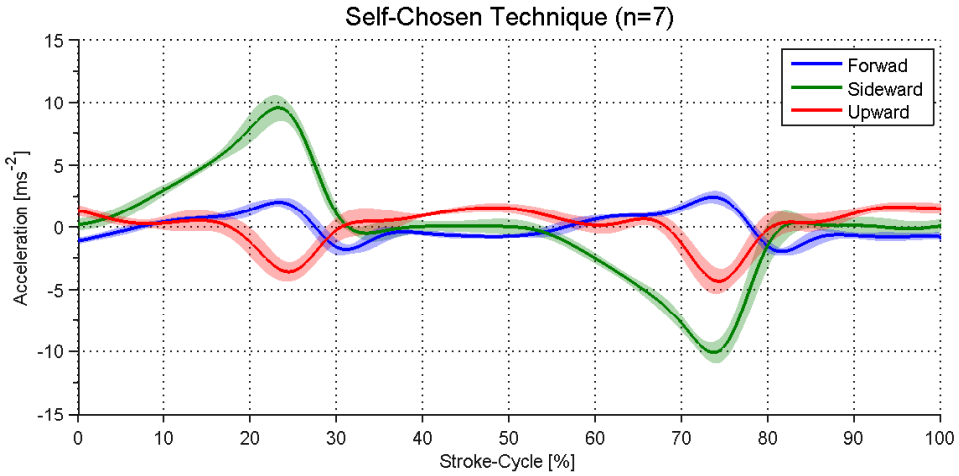

Figure G.2: Velocity during a stroke-cycle of the self-chosen push-off technique, where the colored surface is the standard deviation of the corresponding accelerations.

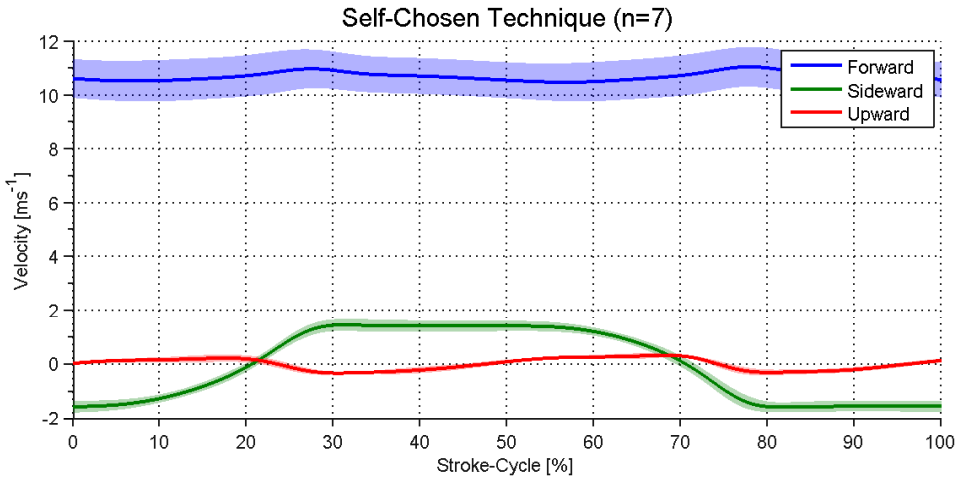

Figure G.3: Velocity during a stroke-cycle of the self-chosen push-off technique, where the colored surface is the standard deviation of the corresponding velocities.

Acceleration and Velocity
The acceleration and velocity pattern in the forward and upward direction were approximately identical for each push-off leg, while the acceleration pattern in the sideward direction was symmetrical (Figure 15.2 and 15.3).

The forward acceleration pattern described the same pattern as the forward power component, while the sideward and upward acceleration patterns were different from their power components. The forward acceleration has limited influence in the forward velocity, due to the high forward velocity.

The sideward acceleration was the highest in magnitude and the peaks were identical but negative. The sideward acceleration has the following pattern: it increased steadily from 0% of the stroke-cycle, peaked around 25%, decreased rapidly to zero acceleration and stayed zero for 15% of the stoke-cycle. The zero acceleration was visible in the velocity plot; the velocity remained constant, while the high acceleration increased the velocity rapidly.

The upward acceleration decreased from the start of the stroke-cycle and was maximally negative at the peak of the sideward acceleration. The acceleration increased until 50% of the stroke-cycle.

G.1.2 Discussion

Power
The forward power component was both positive and negative, while only positive mechanical power in the forward direction was assumed. This was assumed because it is expected that the speed skater only generates a positive force (push-off force in forward direction) and the forward velocity is always positive. The observed negative power can therefore only be the result of overestimation of the friction power. The selected friction estimation method only estimated the friction coefficients as constants during a stroke-cycle. In reality however, the friction changed during a stroke-cycle. The air friction changed due to the movement of the body (Van Ingen Schenau 1982) and the ice friction changes due to the different orientation of the blade on the ice (Houdijk et al. 2001). The used average friction power over or under estimates the friction power during a stroke-cycle. Therefore, the forward power component was distorted during a stroke-cycle and was the study limited to only the average mechanical power during a stroke-cycle. Accurate friction coefficients during a stroke-cycle are required to create an accurate stroke-cycle with this measurement method.

During each repeated pattern, the sideward power component reaches zero power, because the sideward velocity moved from negative to positive. The steady zero power phase was relative long: almost 50% of the stroke-cycle. The speed skater is thus not moving sidewards during half of a stroke-cycle. The sideward power pattern existed thus of burst of sideward power. It was expected that the speed skater was almost constantly moving his/her body sidewards, because the sideward moving pattern is mostly describes as a sinusoidal movement (see next paragraph). This effect was also visible in the sidward velocity. The burst of power were not as high as the forward power, because the sideward velocity was lower, but the acceleration was at least twice as high. During a stroke-cycle, the average sideward power component did not differ much from the forward power component, but the amplitude of the sideward is much lower (Results, Chapter 3).

The upward power component indicated that the body of the skater was constant moving during a stroke-cycle. The power was not high, but the skater was constantly moving. The constant movement of the upper body was expected, since the speed skater assumed to also using his/her weight for a push-off. During a stroke-cycle, the first part of the upward power component is different from the other parts. The reason for this difference is unknown, but it is present in all the push-off techniques (Figure 15.4). It could be the result of the optimization procedure.

The total mechanical power was also negative due to the high influence of the forward power component on the total mechanical power. On average, the forward power component contributed for only 30% of the total mechanical power, but the influence during the stroke-cycle was much higher. This is due to the relative high and low peaks. The total mechanical output was compared to the

result of Fintelman (2011) and Houdijk et al. (2000b). The total mechanical power pattern during a push-off of Fintelman and Houdijk were given in Figure G.4. The mechanical power calculated by Fintelman was only based on the movement in the two-dimensional plane; there were no upward measurements. The shape of Fintelman did have the same characteristics as the measured shape: steep slopes near the peak and the flat slope halfway the push-off. The shape of Houdijk had only the steep slope and did not have the flat slope halfway the push-off. The estimated peaks of both figures, with respect to a guessed mass of $80kg$, are much lower than the measured peaks, $5.5Wkg^{-1}$ and $11Wkg^{-1}$ respectively. The measured peak of the total mechanical power is around $25Wkg^{-1}$. The reason of the high total power component of this study is the most likely the high influence of the forward power component. The high peaks of the forward power component were possibly the results of under estimation of the friction power, but an over estimation of $15Wkg^{-1}$ is maybe to much. The measurements of Fintelman and Houdijk are assumed more accurate, since the power was calculated with the force measurement method (See Appendix A) and did not rely on friction power estimations.

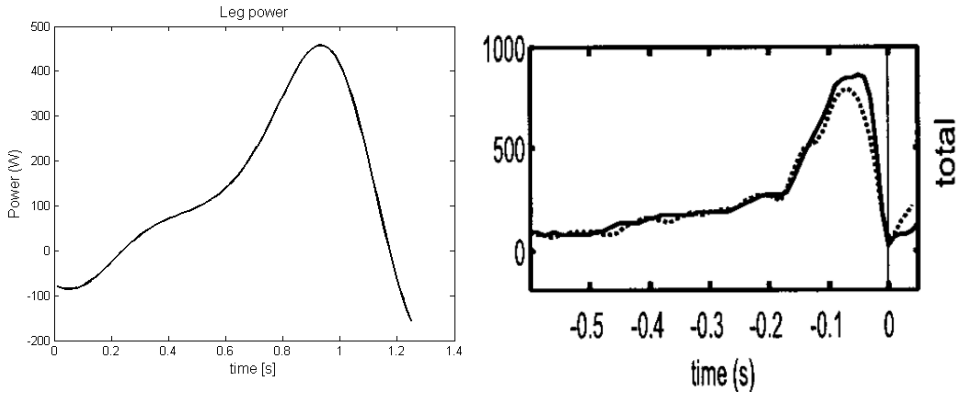

Figure G.4: Mechanical power calculated by Fintelman (2011) (left) and Houdijk et al. (2000b) (right).

Velocity And Acceleration
The asymmetrical push-off acceleration pattern in the sideward push-off were the result of the change of push-off leg, which changes the push-off direction. The sideward accelerations were symmetrical and the forward and upward accelerations display a repeated pattern, because the accelerations were optimized to be identical or symmetrical (Appendix D). To the author's knowledge, accelerations in the forward, sideward and upward direction during a push-off are not reported in literature. However, Van der Kruk (2013b) reported measurements and modeling of the velocity in forward and sideward direction (Figure G.5). The forward velocity describes the same small change in velocity during a stroke-cycle, but it cannot be concluded if the frequency of the pattern is equal: Van Der Kruk did not divide the data into stroke-cycles. The sideward velocity did described a different sinusoidal movement as expected and reported by Van Der Kruk. The sideward velocity of Van Der Kruk described the expected sinusoidal movement. The sideward velocity reported by this study was not a sinusodial movement, but was more flat and had rapid change in velocity. The reason why the sideward velocity described a different pattern is unknown.

G.2 Comparison of Push-off Techniques

The patterns of forward, sideward and upward power components during the stroke-cycle were comparable, but there were some distinct differences in the peaks (Figure G.6). The push-off peaks for each push-off technique occurred at approximately at same point of the push-off. The total mechanical power described the same pattern as the forward power component and is therefore not separately analyzed. To the knowledge of the author, no literature on the forward, sideward and upward mechanical power components is available for comparison.

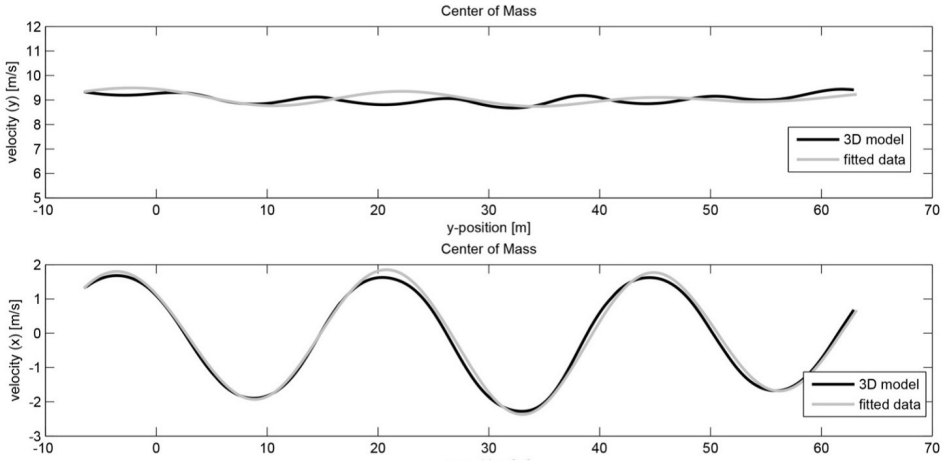

Figure G.5: Forward and sideward velocity by Van der Kruk (2013b).

The forward power peaks were during the small push-off technique higher than the self-chosen technique, while the peaks were lower with the wide push-off technique. In addition, the peaks were also lower for the small push-off and higher for the wide push-off. The main difference between the peaks in the forward mechanical power were the peaks and valleys. The higher and lower peaks with the small and wide push-off technique were also expected, because the push-off is expected to be executed faster or slower. The lower and higher valleys were not expected. It was expected that the lowest peak in the forward power component was the result of only friction, which was approximately equal for each technique.

The sideward power pattern stayed the same, only the peaks change in amplitude. The sideward peaks does increase and decrease to the self-chosen technique for the small and wide push-off, respectively. This was also expected, since a wider movement is the result of an increase in power in the sideward direction.

The upward pattern was almost identical for each push-off technique, but there is an exception for the first part of the stroke-cycle. The first part of the stroke-cycle should be identical with the other parts of the stroke-cycle. It is strange that all of the techniques describe the same difference in the first part of the stroke-cycle. The reason for this difference is unknown, but could be due to the optimization technique used.

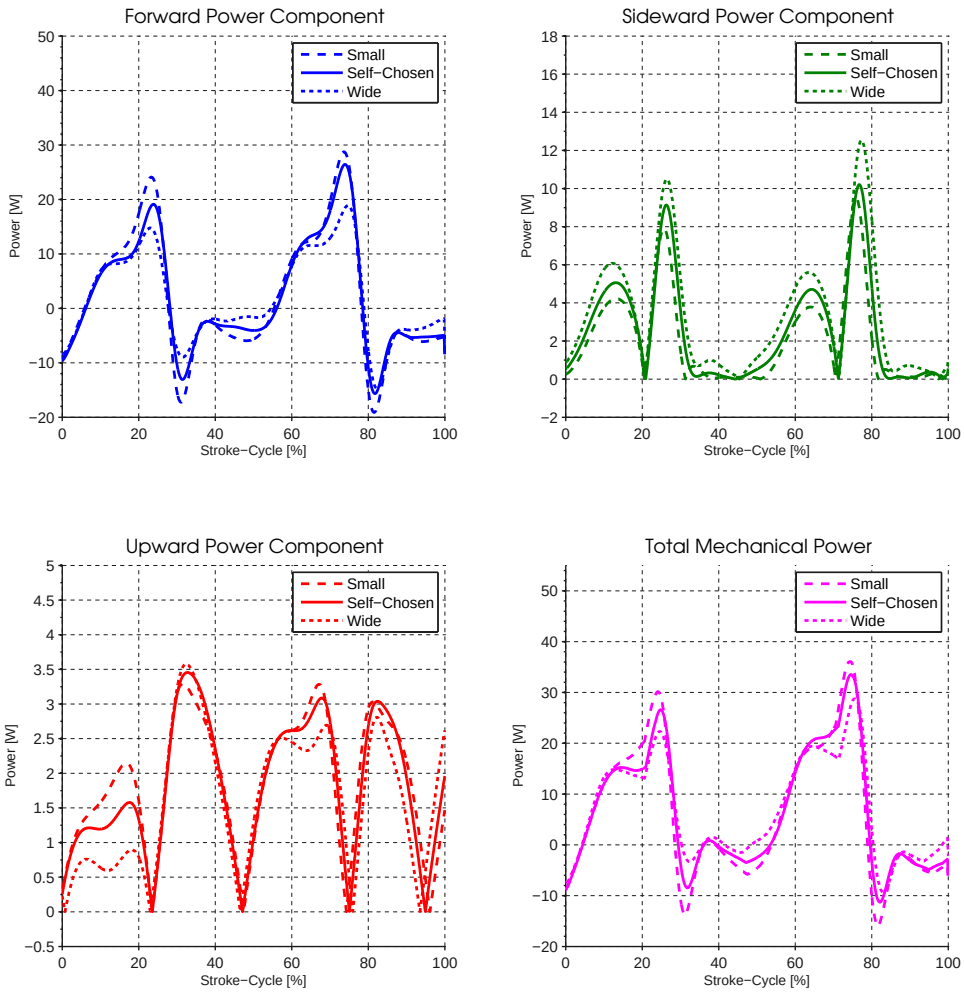

Figure G.6: Power components and total power of the small, self-chosen and wide push-off technique during a stroke-cycle.